**The Thesis Committee for Wendi Liu**
**Certifies that this is the approved version of the following thesis**

# Reservoir fluid characterization and optimization of condensate banking treatment with dimethyl ether in the shale gas condensate reservoir

**APPROVED BY**
**SUPERVISING COMMITTEE:**

**Supervisor:**

Kamy Sepehrnoori

Reza Ganjdanesh

# Reservoir fluid characterization and optimization of condensate banking treatment with dimethyl ether in the shale gas condensate reservoir

**by**

**Wendi Liu**

**Thesis**

Presented to the Faculty of the Graduate School of

The University of Texas at Austin

in Partial Fulfillment

of the Requirements

for the Degree of

**Master of Science in Engineering**

**The University of Texas at Austin**

**August, 2018**

# Dedication

To my parents, for their unconditional love and support.

# Acknowledgements

First of all, I would like to express my sincere gratitude to my supervising professor, Dr. Kamy Sepehrnoori for his guidance in my research and all the help he provided. I also wish to express my appreciation to the second reader of my thesis, Dr. Reza Ganjdanesh, for all his useful suggestions and help. I would like to thank Dr. Abdoljalil Varavei, Bruno Fernande, Yusuf Nasir, and Mehran Mehrabi, for their helpful technical discussion about the problems I encountered, and Dr. Wei Yu, for his useful comments.

Furthermore, I want to thank my beloved families and my boyfriend, for their unconditional love and support, as well as their encouragement and patience for me when I encountered difficulties. Also, I would like to extend my gratitude to all of my friends and officemates. Thanks to their companionship, the days in my graduate school are so memorable. Last but not least, thank all the staffs of the Hildebrand Department of Petroleum and Geosystem Engineering for their efforts to make PGE such a lovely place to work and learn.

# Abstract

## Reservoir fluid characterization and optimization of condensate banking treatment with dimethyl ether in the shale gas condensate reservoir

Wendi Liu, M.S.E.

The University of Texas at Austin, 2018

Supervisor: Kamy Sepehrnoori

As the bottomhole pressure drops below dew point during gas production from hydraulic-fractured shale gas condensate reservoirs, condensate-banking forms near the wellbore and compromises the gas productivity. Dimethyl ether (DME) is used to efficiently mitigate the condensate banking. However, the cost of injecting DME in field scale is one of the challenges hindering its further application. Also, complexity of shale gas condensate reservoir requires the accurate phase behavior model for reliable long-term oil and gas production forecast.

This study investigates the efficiency of DME treatment and optimizes its application based on a rich gas condensate fluid model to obtain the highest net present value (NPV) with different reservoir permeabilities. An in-house simulator, UTCOMP, with a composition-dependent relative permeability model was used for this study. The production rates with and without solvent treatment are compared to determine the benefit of DME injection. The effectiveness of DME is also evaluated for rich and lean gas

condensate reservoirs and rich gas condensate reservoirs with different permeabilities. The result proves the eligibility of DME removing the blockage for different types of reservoir fluids and reservoirs with very low permeabilities. It also indicates that slug size would affect the efficiency of DME mixture ratio and reinjection. Therefore, further simulation is proposed to analyze the impact from the amount of DME on NPV at varying permeabilities for one-time injection. The practical optimum strategies in this study make it possible to inject DME for shale gas production economically.

# Table of Contents

# List of Tables

# List of Figures

# Chapter 1: Introduction

## 1.1 Problem statement and objectives of the study

For a gas condensate reservoir, hydrocarbon resides be in gas phase at initial reservoir condition. As production continues and pressure depletes to the dew point, liquid phase would start to form. The liquid saturation would build up near the wellbore, which is called condensate-banking problem. Also, during hydraulic fracturing in a tight reservoir, fracturing fluid would also cause the water blockage problem. Solvent injection has proven its efficiency in treatment of liquid banking. Compared with gas injection, solvents like methanol or ethanol is not only miscible with condensate but also with water, so it can remove condensate and water block at the same time. In this study, dimethyl ether (DME) is proposed as a better treatment because of its high vapor pressure, hence, DME would flow back more quickly compared with other alcohol. An in-house compositional simulator with robust three phase flash calculation is used to investigate the efficiency of DME treatment for rich and lean gas condensate fluid and optimize it in the cases with different permeabilities.

## 1.2 Organization of the chapters

Chapter 2 is the literature review covering the previous work on the reservoir fluid characterization, the difficulties of production in gas condensate reservoir, the banking formation and treatment simulation with the compositional simulator, UTCOMP.

Chapter 3 presents the phase behavior model and simulation model for the cases in the thesis. The phase behavior model was based on the actual rich gas condensate fluid data and the EOS parameters were tuned to match the PVT experiments data with CMG-Winprop.

Chapter 4 shows results of the case study and the mechanism of DME removing condensate banking is also explained in this chapter. The effectiveness of DME treatment was testified on both rich and lean gas condensate fluids. Then, the optimum NPV was discussed for rich gas condensate case at the reservoir permeability range from 100 nd to 1000 nd.

Chapter 5 covers the conclusions from this study and possible future directions were proposed.

# Chapter 2: Literature Review

## 2.1 Reservoir Fluid Characterization

Phase behavior of the condensate mixture plays an essential role in compositional simulation of gas condensate reservoir. Proper fluid characterization is a vital step to get the accurate phase behavior in the compositional simulator. Reservoir fluid characterization includes the major steps as following: acquisition of representative samples, pressure-volume-temperature (PVT) measurements from the reliable service laboratories, quality control (QC) procedures to make sure data quality, and development of equation of state (EOS) models to accurately capture the change of fluid properties as function of pressure, temperature and composition. (Pedersen et al., 2014) This chapter mainly discussed about the part of EOS tuning and match the phase behavior after acquiring the PVT data from the laboratory.

### 2.1.1 PVT experiments for gas condensate mixtures

PVT properties is the general term that is used to describe the volumetric behavior of a reservoir fluid as a function of pressure and temperature. An essential PVT property is the saturation pressure at reservoir temperature. Once the reservoir pressure reaches the saturation pressure, a second phase starts to form and the composition of the produced well stream will change. It is customary to use the volumes of oil and gas at atmosphere pressure (1 atm or 1.01325 bar) and 15 $^{o}$C as reference values.

#### *2.1.1.1 Constant composition expansion experiment*

The constant composition expansion experiment is sketched for the gas condensate mixture in **Figure 2-1** (Pedersen et al., 2014). A known volume of single phase sample is charged to a windowed PVT cell and heated to the experimental temperature. At this temperature, the fluid is stabilized at a pressure above reservoir pressure and saturation

pressure. As the pressure decreases, the dew point pressure can be visually measured. The relative volume as defined in Equation (1) can be obtained at all pressures. The gas phase compressibility factor as defined in Equation (2) is recorded for pressures above the saturation pressure. Below the saturation pressure, the liquid volume as a percentage of the saturation point volume is reported in Equation (3).

$$V^{rel} = \frac{V^{tot}}{V^{sat}} \quad (1)$$

$$Z = \frac{PV}{RT} \quad (2)$$

$$\%Liquid\ dropout = 100 * \frac{V^{tot}}{V^{sat}} \quad (3)$$

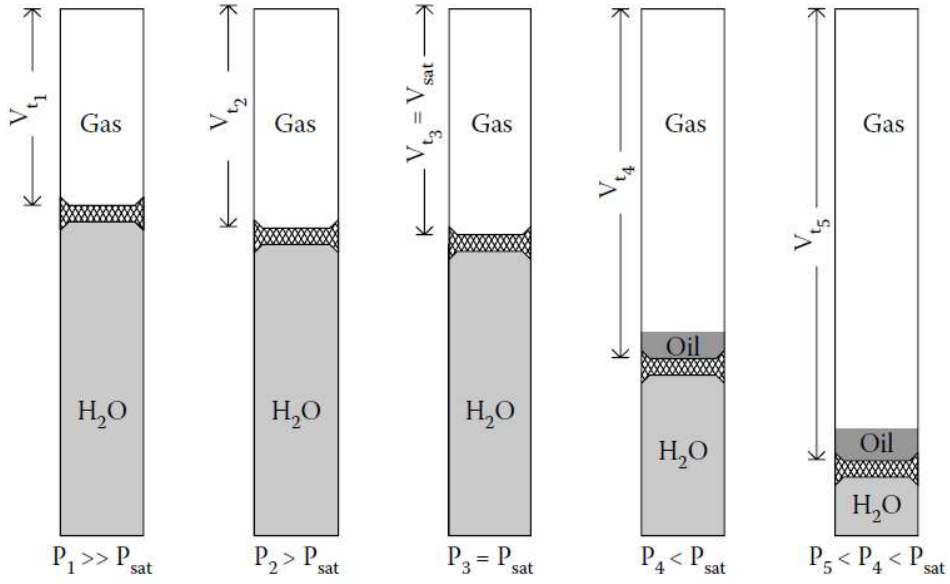


**Figure 2-1**: Schematic of a constant composition expansion experiment for gas condensate

### *2.1.1.2 Constant volume depletion experiment*

The constant volume depletion experiment is sketched in **Figure 2-2** (Pedersen et al., 2014). The test consists of subsequent pressure expansions and constant pressure displacement of excess volume of gas to return the cell content to a constant volume. The constant volume is equal to the volume at the saturation pressure. The procedure is usually repeated for six stages down to the abandonment pressure of approximately 50 bar.

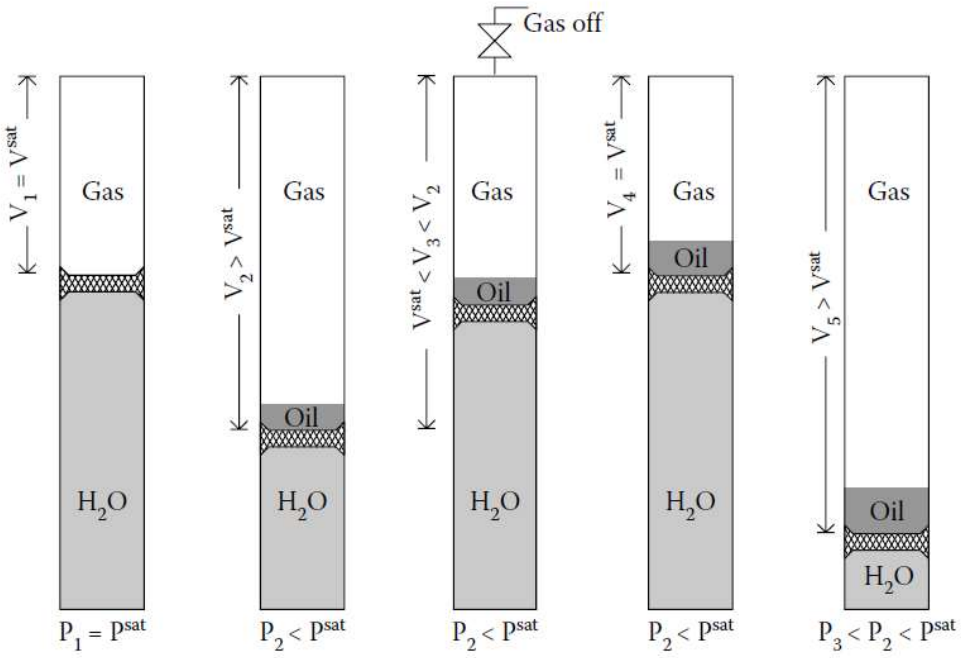


**Figure 2-2**: Schematic of a constant volume depletion experiment

### 2.1.2 Equation of State

The calculation of the PVT relation for the mixture is based on a cubic equation of state. The most famous equation of state is van der Waals equation (van der Waals 1873). And in petroleum industry, the most commonly used EOS is the one proposed by Redlich and Kwong (1949) and Peng and Robinson (1976) then further developed the equation.

#### *2.1.2.1 Van der Waals Equation*

Van der Waals equation was derived using the phase behavior of a pure component from the ideal gas law, where $R$ equal to the gas constant, $T$ the absolute temperature, and $V$ the molar volume.

$$P = \frac{RT}{V} \qquad (4)$$

While the molar volume of the component at high pressures is not zero as ideal gas law expected, the volume in van der Waals equation is corrected by add the b-parameter as follows:

$$V = \frac{RT}{P} + b \qquad (5)$$

Which would give the following expression for $P$:

$$P = \frac{RT}{V-b} \qquad (6)$$

Another term considering the attractive force which is proportional to $\frac{1}{V^2}$ is then added to the pressure:

$$P = \frac{RT}{V-b} - \frac{a}{V^2} \qquad (7)$$

Here comes the final form of the van der Waals equation. The constants $a$ and $b$ are equation of state parameters, the value of which are determined by evaluating the critical isotherm curve. At the critical point,

$$\left(\frac{\partial P}{\partial V}\right)_{T\ at\ T=Tc,P=Pc} = \left(\frac{\partial^2 P}{\partial^2 V^2}\right)_{T\ at\ T=Tc,P=Pc} = 0 \qquad (8)$$

The molar critical volume $Vc$ is related to $Pc$ and $Tc$ by the correlation above and van der Waals equation. After the five constants ($Tc$, $Pc$, $Vc$, $a$ and $b$) enter into the equations and eliminate $Vc$, the following expression for $a$ and $b$ can be derived.

$$a = \frac{27R^2T_C^2}{64Pc} \qquad (9)$$

$$b = \frac{RT_c}{8P_c} \qquad (10)$$

### *2.1.2.2 Redlich-Kwong Equation*

Redich and Kwong equation takes the form,

$$P = \frac{RT}{V-b} - \frac{a}{\sqrt{T}V(V+b)} \quad (11)$$

It can be seen that the attractive term has a more complicated temperature dependence by comparing the equation with van der Waals equation. The temperature dependent term helps to improve the vapor pressure predictions. The constant $a$ and $b$ can be obtained from imposing the critical point criteria expressed in the same way as did in van der Waals equation.

$$a = \frac{0.42748\ \ {}^{2}T_C^{2.5}}{Pc} \quad (12)$$

$$b = \frac{0.08664RT_c}{Pc} \quad (13)$$

For a mixture with $N$ components, parameters $a$ and $b$ can be found using the mixing rules as following:

$$a = \sum_{i=1}^{N}\sum_{j=1}^{N} Z_i Z_j a_{ij} \quad (14)$$

$$b = \sum_{i=1}^{N} Z_i b_i \quad (15)$$

In which $Zi$ and $Zj$ are the mole fractions of component $i$ and $j$, respectively. The term $a_{ij}$ and $b_i$ can be found from the following,

$$a_{ij} = \frac{0.42748R^2T_{Cij}^{2.5}}{Pcij} \quad (16)$$

$$b = \frac{0.08664RT_{ci}}{Pci} \quad (17)$$

In which $T_{cij}$ is related to the pure component critical temperatures $T_{ci}$ and $T_{cj}$ of the components $i$ and $j$ as follows,

$$T_{cij} = \sqrt{T_{ci}T_{cj}}(1 - k_{ij}) \quad (18)$$

In which $k_{ij}$ is a binary interaction parameter for components $i$ and $j$. $P_{cij}$ can be found from

$$P_{cij} = \frac{Z_{cij}RT_{cij}}{V_{cij}}, \quad (19)$$

where

$$Z_{cij} = \frac{Z_{ci}+Z_{cj}}{2} \quad (20)$$

and

$$V_{cij} = \left(\frac{V_{ci}^{\frac{1}{3}}+V_{cj}^{\frac{1}{3}}}{2}\right)^3. \quad (21)$$

$Z_{ci}$ and $Z_{cj}$ are the compressibility factor of the pure component $i$ and $j$ at their critical points, respectively.

#### *2.1.2.3 Soave-Redlich-Kwong Equation*

Soave (1972) proposed to replace the term $\frac{a}{\sqrt{T}}$ in the RK equation by a more general temperature dependent term, $a(T)$ to further improve the vapor pressure accuracy from RK equation.

$$P = \frac{RT}{V-b} - \frac{a(T)}{V(V+b)} \quad (22)$$

#### *2.1.2.4 Peng-Robinson Equation*

To correct the lower liquid phase densities predicted by SRK equation, Peng-Robinson equation traced the deficiency by correcting the pure component critical compressibility factor. The Peng-Robinson equation is in the following form:

$$P = \frac{RT}{V-b} - \frac{a(T)}{V(V+b)+b(V-b)}, \quad (23)$$

where

$$a(T) = a_c \alpha(T), \quad (24)$$

$$a_c = \frac{0.45724 \mathrm{R}^2 T_C^2}{Pc}, \quad (25)$$

$$\alpha(T) = \left(1 + m\left(1 - \sqrt{\frac{T}{Tc}}\right)\right)^2, \quad (26)$$

$$m = \begin{cases} 0.37464 + 1.54226\omega - 0.26992\omega^2 & For\ \omega < 0.49 \\ 0.379642 + 1.48503\omega - 0.164423\omega^2 + 0.016666\omega^3 & For\ \omega > 0.49 \end{cases}, \quad (27)$$

$$b = \frac{0.07780 \quad c}{Pc}, \quad (28)$$

and where $\omega$ is the acentric factor.

### 2.1.3 $C_{7+}$ Characterization and Lumping

To use the EOS for phase equilibrium calculation on a fluid compositional model, the critical temperature, the critical pressure and the acentric factor are required for each component in the mixture as well as the binary interaction parameter. Naturally occurring oil or gas condensate mixtures can contain more than thousands of components, which is a

too high number to do the calculation. Therefore, some components must be lumped as pseudo-components. $C_{7+}$ represents the hydrocarbons with seven and more carbon atoms and is lumped as a pseudo-component to find the necessary EOS parameters.

Lumping is supposed to consist of the two parts: deciding what carbon number fractions to lump into the same pseudo-component, and averaging $Tc$, $Pc$, and $\omega$ of the individual carbon number fractions to those representative for the whole lumped pseudo-component. Khan et al. (1992) proposed a lumping scheme as following: group nonhydrocarbons separately, make three separate groups of hydrocarbons from C1 to C6, and divide $C_{7+}$ fractions into three or more groups on a weight basis of approximately equal size. And there are heuristic guidelines for lumping:

- Neglect nonhydrocarbons with mole fractions less than 0.005 unless it is the nonhydrocarbon that is injected.
- C1-C6 are grouped as $C_1$, $C_{2\text{-}3}$, and $C_{4\text{-}6}$. But there could be other combinations depending on the respective mole fractions.
- The number of pseudo-components for splitting $C_7$+ fractions is determined from its mole fractions as following

| C7+ mole fraction | NO. of Pseudo-components |
|---|---|
| <0.05 | 1 |
| 0.05-0.4 | 2 |
| 0.4-0.6 | 3 |
| 0.6-0.8 | 4 |
| >0.8 | 5 |

### 2.1.4 Flash and Phase Envelope Calculations

From a flash calculation, we can know the number of phases and the molar compositions of each phases with the provided pressure, temperature and mole fractions in two phase equilibrium.

$$K_i = \frac{y_i}{x_i} = \frac{\varphi_i^L}{\varphi_i^V} \qquad i = 1, 2, \dots, \mathrm{N} \qquad (29)$$

$$\sum_{i=1}^{N}(yi - xi) = \sum_{i=1}^{N} \frac{zi(Ki-1)}{1+\beta(Ki-1)} = 0 \qquad i = 1, 2, \dots, \mathrm{N} \quad (30)$$

where $x_i$ is the mole fraction of component $i$ in the liquid phase, $y_i$ is the mole fraction of component $i$ in the vapor phase, $\varphi$ is the fugacity coefficient and $K_i$ is the equilibrium ratio also called K-factor of component $i$.

For a pure component, two phase equilibrium can only exist at the vapor pressure and vapor pressure may be determined from a cubic EOS but in an iterative manner. For mixtures with two or more components, it is necessary to first locate mixture saturation pressures before considering the general PT-flash problem.

A phase envelop can be calculated by performing a series of saturation point calculations but it may be very time consuming and probably lead to convergence problems near the critical point. The procedure proposed by Michelsen (1980) is used instead.

## 2.2 Compositional Simulation for Gas Condensate Reservoir

### 2.2.1 Treatment on Gas Condensate Reservoir

The retrograde condensation phenomena are one kind of mixture behavior that liquid forms with an isothermal decrease in pressure or an isobaric increase in temperature. For a gas condensate reservoir, the reservoir fluid is a single phase fluid at original reservoir condition and the primary component is methane (C1). The solution gas oil ratio (GOR) of

a gas condensate reservoir is typically between 3000 and 150,000 SCF/STB and liquid gravities between 40 and 60° API (Standing 1977). As the drawdown pressure drops below the dew point, condensate liquid saturation would build up near the well and restrict the flow of gas. The well productivity therefore is decreased due to the reduction in the gas relative permeability (Pope et al. 2000). Another reason to the loss of productivity can be the formation water trapped as an immobile phase near the wellbore. The blockage occurs not only in conventional reservoir, but also shale gas condensate reservoir with hydraulic fractures. Bang et al. (2008) showed that condensate blockage along fractures can significantly reduce the productivity of fractured wells. And much of the fracturing fluid would be trapped in small pore of the tight formations during fracturing (Gupta 2009). The trapped water would increase the water saturation near fractures and lower the relative permeability of hydrocarbon phases and impairs production rates (Bertoncello et al. 2014).

So far, a large amount of work has been done to improve the condensate recovery and mitigate the blockage to gas production. Chemical treatment can be used for wettability alternation to help gas production by improving the gas relative permeability (Bang et al. 2010). Sayed et al. (2018) proposed a novel surface modified nanoparticles as an efficient way of wettability alternation. Also, Huff-n-puff gas injection can be an effective way by maintaining the pressure above dew point and prevent liquid phase formation, like $CO_2$ or $N_2$ injection. Gas injection helps revaporize the condensate to gas phase again to recover the liquid (Meng and Sheng 2016). Meanwhile, solvent injection has been shown the efficiency in mitigating the liquid banking especially water blocks that gas injection is not capable of removing. Bang et al. (2010) tested the phase behavior of methanol (MeOH) and isopropanol (IPA) with mixtures of hydrocarbons and water at reservoir condition. MeOH (Al-Anazi et al. 2005) has been proved as a successful solvent in field application to remove the condensate blockage in the Hatters's Pond field in Alabama. Dimethyl ether

(DME) was introduced as a better treatment for the first time for liquid blocks compared with Methanol and Ethanol in hydraulic fractured shale gas condensate reservoir (Ganjdanesh et al. 2016). DME is miscible with both condensate and water at reservoir condition and can flow back faster compared with glycols and light alcohols due to its higher vapor pressure. More complex mixing rule has been investigated to improve the accuracy of modeling the phase behavior of the solvent mixture by Ratnakar et al. (2017). As DME is miscible with condensate and also easily partitions into aqueous phase, a three phase flash calculation is necessary to model the phase behavior of the mixture during injection and flowback. However, the major changes in phase behavior of reservoir fluids cannot be captured by most of commercial simulators without robust three phase flash calculation option. The importance of using the three-phase model over the two phase model was demonstrated with the Eagle Ford gas condensate mixture by Neshat et al. (2018). And most commercial simulators use density of each phase as a way of phase identification, which is not reliable and would mislabel phases. The mislabeling of phases in simulation would lead to discontinuity in relative permeability. Perschke (1988) implemented a phase identification approach with a three phase flash based on tracking a key component. This method was used to assign relative permeability to each phase in a consistent way. But it did not account for the change of the relative permeability with composition except for the capillary number effect. Neshat and Pope (2017) included the hysteresis effect in their relative permeability model by coupling with capillary pressure model for multiphase flow problems. The robustness of their model was demonstrated with the solvent simulation for liquid blockage problem in unconventional formations.

### 2.2.2 Compositional Simulation with UTCOMP

In this thesis, a compositional three phase flash simulator, UTCOMP (Chang 1990), was used to simulate the stimulation process, which is a non-isothermal, three-dimensional, implicit in pressure and explicit in phase saturations and compositions (IMPEC). UTCOMP solves the mass-conservation equation for all components with respect to time to obtain the distribution of phases and fluid species in the reservoir. Next step is to determine the number and amount of hydrocarbon phases and phase compositions using the Peng-Robinson equation-of-state. Stability analysis is performed prior to the flash calculation to determine the number of equilibrium phases evolving from the mixture at a given pressure, temperature, and fluid composition. Once UTCOMP completes the flash calculation, phase properties are updated, and consequently, phase saturations are calculated. The phase saturations are then used to determine the relative permeabilities and capillary pressure.

The solvent injection causes major changes in the phase behavior with phases appearing and disappearing during injection and flow back. These changes cannot be captured by simulators without a robust phase labeling. If one phase is mislabeled in one timestep, the relative permeability of that phase between the two time steps would be discontinuous. This discontinuity often reduces the time step size and causes the simulation to slow down or stop as well as being physically incorrect. A composition-dependent relative permeability model developed by Yuan and Pope (2011) is used in this method. The Peng-Robinson equation-of-state is used to calculate the Gibbs free energy of all three phases. Interpolation is used to calculate the relative permeability parameters such as residual saturations, end-point relative permeability, and Corey exponents based on the measured reference values for each phase at a specific composition, pressure and temperature. **Figure 2-3** (Yuan and Pope 2011) shows a schematic of how the end-point

relative permeability parameter is interpolated. A simplified Corey-type model was used to calculate the relative permeability of each phase using the interpolated relative permeability parameters. This approach results in relative permeability values that are independent of the phase numbers from flash calculations. Therefore, mislabeling does not affect the continuity of phase relative permeability. The relative permeability parameters for reference phases used in this study are summarized in **Table 2-1**.

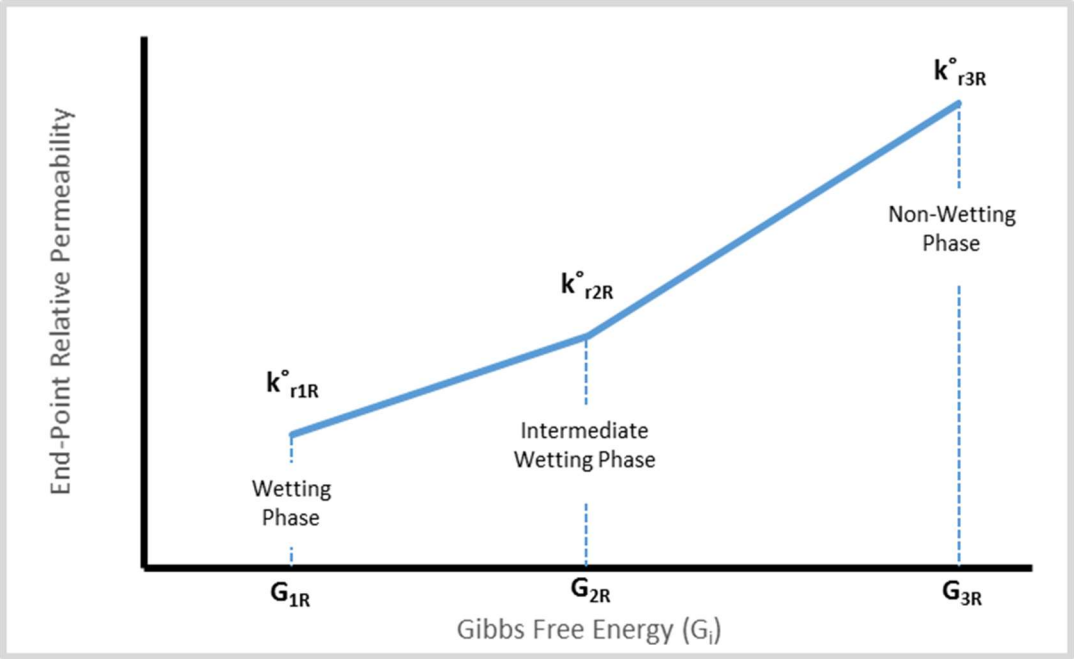

**Figure 2-3**: Schematic of the end point relative permeability as a function of Gibbs free energy

| | Oil | Gas | Aqueous |
|---|---|---|---|
| $\boldsymbol{k_{rj}^{\circ}}$ | 0.6 | 0.6 | 0.2 |
| $\boldsymbol{S_{jr}}$ | 0.25 | 0.25 | 0.2 |
| $\boldsymbol{n_j}$ | 2.0 | 2.0 | 3.0 |

**Table 2-1**: Reference parameters for relative permeability model used in the simulation of solvent treatment

# Chapter 3: Model

## 3.1 Phase Behavior Model

Gas condensate in shale formations is known as liquid-rich shale (LRS) reservoirs. It is essential to model pressure/volume/temperature (PVT) properly to get accurate short and long term LRS production simulation results. This study presented two phase behavior models based on two types of fluids. Based on the condensate/gas ratio of each fluid, one can be considered as rich gas condensate (with condensate/gas ratio 107 STB/MMSCF) and the other one is lean gas condensate (with condensate/gas ratio 12.8 STB/MMSCF) (Dindoruk 2012). This study will illustrate how to derive EOS parameters of the rich gas condensate fluid from field data and matching the saturation pressure, constant composition expansion (CCE) and constant volume depletion (CVD) experiments in detail in this session.

### 3.1.1 Characterization of Rich Gas Condensate fluid

CMG-Winprop (2016) is an Equation of State (EOS) based fluid behavior and PVT modeling simulator. Winprop is capable of tuning an equation of state to match the laboratory fluid data and predicting a phase behavior model for the simulation with UTCOMP. The supplied data is from the rich shale gas condensate reservoir and contains a description of the composition, saturation pressure, CCE and CVD experiments results used for tuning the EOS to match the fluid behavior. The EOS tuned for the phase behavior model in the thesis is Peng-Robinson EOS.

Before lumping the reservoir composition into pseudo components, it is necessary to match the saturation pressure first. In particular, the values associated with the heaviest component can be uncertain. Therefore, future tuning of the EOS would be easier if an

initial match is obtained before combining components and their properties into pseudo-components.

Depending on the experimental data to be matched, various EOS parameters may have an impact on the phase behavior while others may not. In this case, in order to match the saturation pressure, the critical pressure (Pc) and critical temperature (Tc) can be changed. Specifically, the parameters with the most uncertainty should be the ones that are altered.

There are over 30 components in the rich gas condensate reservoir fluid. Usually it is not feasible to run models with such amount of components. Therefore, a method to avoid long run times is to lump similar components into pseudo-components. Pseudo-components consist of properties from the components that they are defined from. However, the components have internal interactions that would no longer be accounted for once lumped together. As such, regression is usually done after lumping components to tune the EOS to laboratory data. Proper lumping scheme has been discussed in session 2.1.2.

It is essential to re-match the saturation pressure due to the lumping occurred. Lumped component properties are a function of the properties of the components which comprise them. Internal interactions between these components in the pseudo-components made make them not directly represent the behavior of the components. **Table 3-1** shows the saturation pressure of the rich gas condensate fluid obtained from constant composition expansion test and the matched saturation pressure before and after lumping. The error of the matched saturation pressure before lumping is 1.78% and that after lumping is 2.83%. Therefore, it is often necessary to tune the properties of pseudo-components to achieve appropriate matches to experimental data.

| Experimental Saturation Pressure (psia) | Matched Saturation Pressure before lumping (psia) | Matched Saturation Pressure after lumping (psia) |
|---|---|---|
| 4313 | 4390 | 4191.36 |

**Table 3-1**: Comparison between the saturation pressure obtained from constant composition expansion test and the matched saturation pressure from CMG-Winprop at 239 $^{o}$F before and after lumping

The constant composition expansion test was added to CMG-Winprop to match the laboratory result to evaluate the current EOS modelling. **Figure 3-1** compares the simulated and experimental results of constant composition expansion test. **Figure 3-2** compares the simulated and experimental results of constant volume depletion test. It is obvious that the results are close enough and there is no significant discrepancy. Therefore, the EOS parameters obtained from CMG-Winprop simulation can reflect the fluid behavior quite accurately.

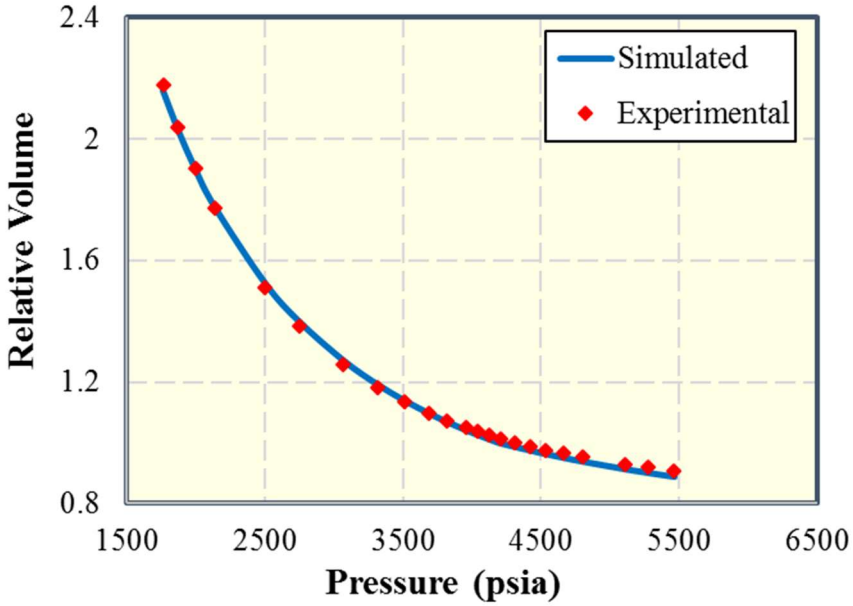
Simulated
Experimental
Relative Volume
2.4
2
1.6
1.2
0.8
1500
2500
3500
4500
5500
6500
Pressure (psia)

(a)

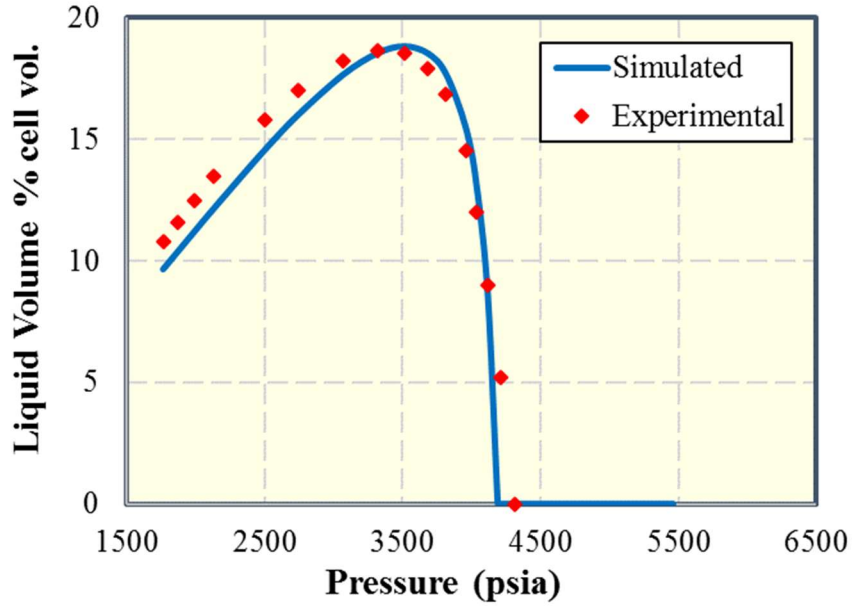
Simulated
Experimental
Liquid Volume % cell vol.
20
15
10
5
0
1500
2500
3500
4500
5500
6500
Pressure (psia)

(b)

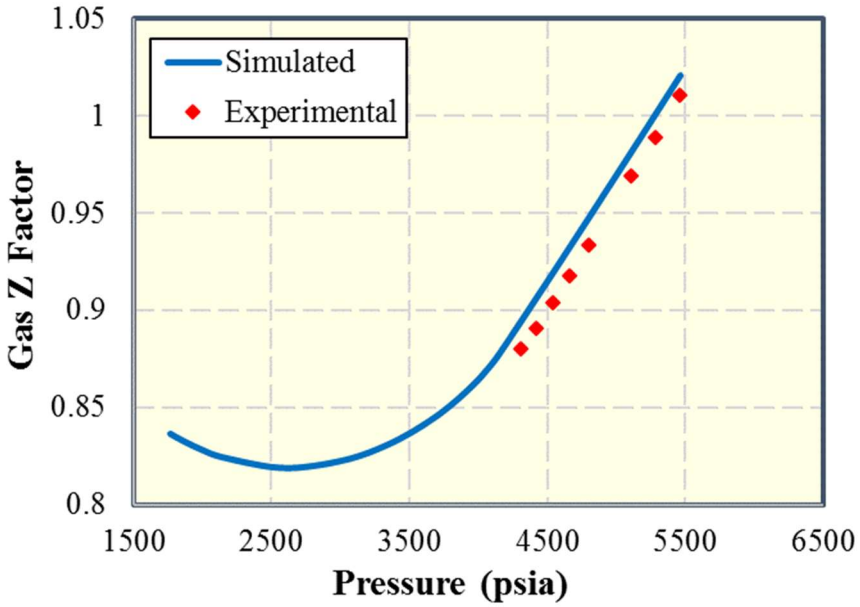


(c)

**Figure 3-1**: Comparison of (a) relative volume (b) liquid dropout (c) gas z factor at different pressure between simulated and experimental results

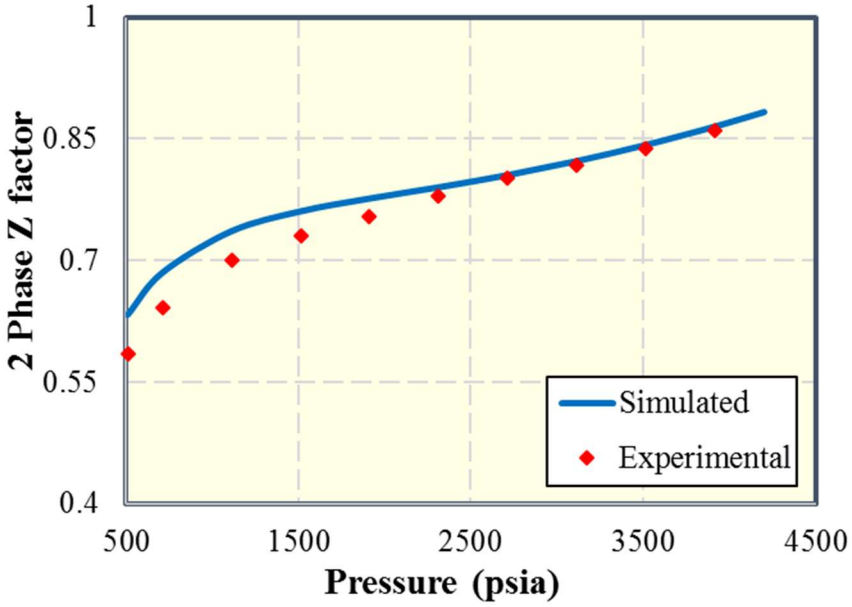


(a)

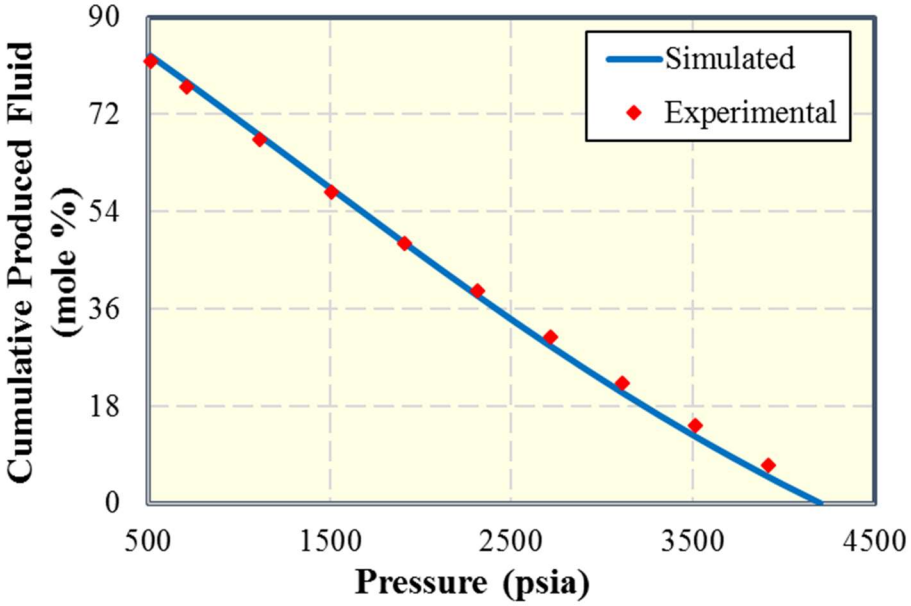


(b)

**Figure 3-2**: Comparison of (a) 2 phase Z factor (b) cumulative produced fluid at different pressure between simulated and experimental results

### 3.1.2 Phase Behavior Model Used for Simulation

The composition and Peng-Robinson equation of state (EOS) (Peng and Robinson 1976) parameters used in the following reservoir simulation are given in **Tables 3-2** and **3-3**. The binary interaction coefficients (BIC) between hydrocarbons were set to be zero. The BICs for DME/water, DME/hydrocarbon and the lean gas fluid compositions were obtained from literature (Ganjdanesh et al., 2016). The number of pseudo-components was determined based on the fluid composition as the lumping scheme from Khan et al. (1992). EOS parameters of the rich condensate fluid were obtained from CMG-Winprop simulation as discussed in session 3.1.2. **Figure 3-3** shows the two phase envelop of the rich gas condensate fluid and the lean gas condensate fluid. **Figure 3-4** shows the liquid dropout of both fluids at different pressure.

| | Initial Composition (mol%) | Critical pressure (psi) | Critical temperature (R) | Critical volume ($ft^3$/lb m-mol) | Molar weight (lb/lbm-mol) | Acentric factor | Parachor coefficient | BIC with respect to DME |
|---|---|---|---|---|---|---|---|---|
| $H_2O$ | 57.014 | 3197.85 | 1165.14 | 0.985 | 18.02 | 0.344 | 52.00 | -0.170 |
| $N_2$ | 0.377 | 492.32 | 227.16 | 1.437 | 28.01 | 0.040 | 41.00 | 0.100 |
| $CH_4$ | 29.141 | 667.20 | 343.08 | 1.590 | 16.04 | 0.008 | 77.00 | 0.290 |
| $C_2$ | 5.250 | 42.54 | 363.30 | 0.197 | 42.82 | 0.143 | 145.20 | 0.250 |
| $C_3$-$C_4$ | 3.895 | 33.76 | 511.56 | 0.334 | 83.74 | 0.247 | 250.00 | 0.250 |
| $C_5$-$C_8$ | 2.714 | 30.91 | 579.34 | 0.406 | 105.91 | 0.286 | 306.00 | 0.200 |
| $C_{9+}$ | 1.610 | 21.58 | 788.74 | 0.921 | 200.00 | 0.687 | 686.30 | 0.075 |
| DME | 0.000 | 789.39 | 720.51 | 2.851 | 46.07 | 0.200 | 132.74 | 0.000 |

**Table 3-2**: Initial composition and Peng-Robinson EOS for mixture of the rich gas condensate fluid, water and DME

| | Initial Composition (mol%) | Critical pressure (psi) | Critical temperature (R) | Critical volume ($ft^3$/lb m-mol) | Molar weight (lb/lbm-mol) | Acentric factor | Parachor coefficient | BIC with respect to DME |
|---|---|---|---|---|---|---|---|---|
| $H_2O$ | 50.000 | 3197.85 | 1165.14 | 0.985 | 18.015 | 0.344 | 52.000 | -0.170 |
| $N_2$ | 0.198 | 492.32 | 227.16 | 1.437 | 28.013 | 0.040 | 41.000 | 0.100 |
| $CH_4$ | 36.882 | 667.20 | 343.08 | 1.590 | 16.043 | 0.008 | 77.000 | 0.290 |
| $C_2$ | 7.575 | 708.35 | 549.72 | 2.377 | 30.070 | 0.098 | 108.000 | 0.250 |
| $C_3$ | 2.742 | 615.76 | 665.64 | 3.260 | 44.097 | 0.152 | 150.300 | 0.250 |
| $C_4$-$C_6$ | 2.141 | 501.82 | 817.09 | 4.784 | 66.993 | 0.229 | 219.161 | 0.200 |
| $C_{7+}$ | 0.463 | 404.14 | 1322.28 | 9.250 | 116.800 | 0.370 | 335.851 | 0.075 |
| DME | 0.000 | 789.39 | 720.51 | 2.851 | 46.070 | 0.200 | 132.737 | 0.000 |

**Table 3-3**: Initial composition and Peng-Robinson EOS for mixture of the lean gas condensate fluid, water and DME

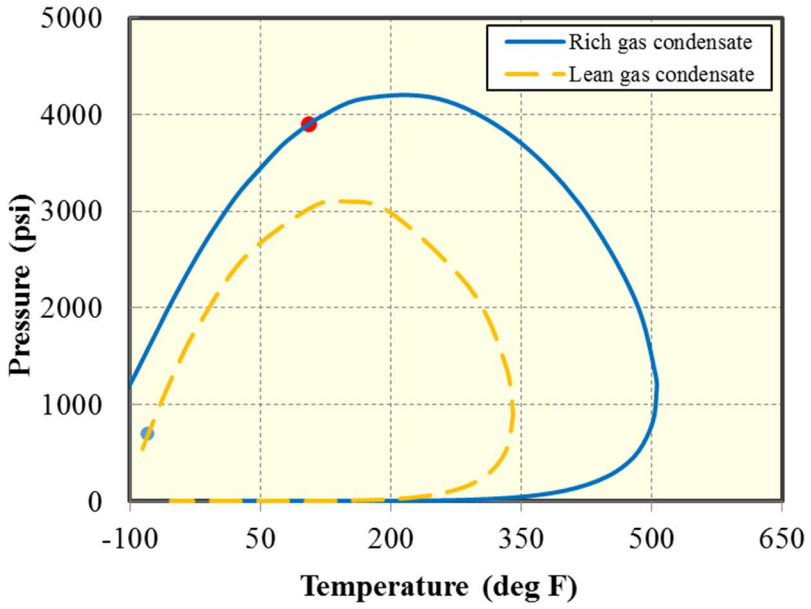


**Figure 3-3**: Two phase diagram of rich and lean gas condensate fluid

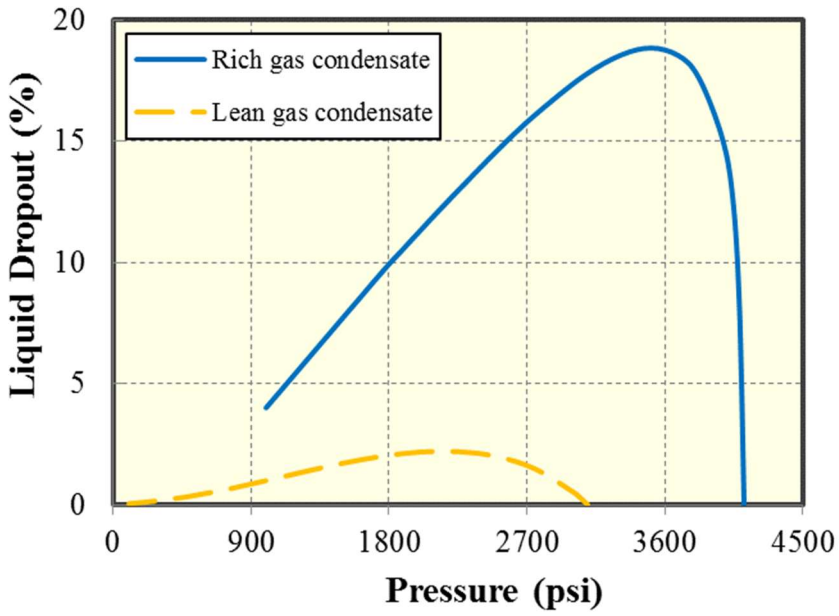


**Figure 3-4**: Liquid dropout for rich and lean gas condensate fluid

### 3.2 Simulation Model

The simulations of the gas condensate reservoir model were performed with an EOS compositional simulator UTCOMP (Chang 1990) with a three phase flash calculation option. The simulation model was built for a 5000×1400×100ft$^3$ rectangular reservoir made up of 50 identical segments. There were 25 transverse fractures evenly distributed along a 5000ft long horizontal wellbore with 200ft fracture spacing. The fracture was planar penetrating entire layer with half-length of 300ft. Since all the segments were identical and symmetrically distributed, only one segment with a half-fracture was modeled and the total production was obtained by multiplying with the number of the segments. It was a 2D model with 33 gridblocks in x direction and 30 gridblocks in y direction and 1 gridblock in z direction simulating one 200×700×100 ft$^3$ segment of the reservoir. The reservoir model is shown in **Figure 3-5**. The reservoir was assumed to be homogeneous and porosity kept constant as pressure changes. Initial water saturation is 20% for rich gas condensate fluid and 19% for lean gas condensate fluid. The reservoir temperature is 239°F for rich gas condensate and 130°F for the lean gas condensate. Both reservoirs kept producing for 600 days with constant flowing bottomhole pressure of 1000 psi. The reservoir and fracture parameters are summarized in **Table 3-4**.

| | |
|---|---|
| Reservoir pressure (psi) | 3100 |
| Depth of the formation (ft) | 5000 |
| Rock porosity | 0.1 |
| Rock permeability (md) | 0.001 |
| Fracture porosity | 0.3 |
| Fracture permeability (md) | 10000 |
| Fracture aperture (ft) | 0.01 |
| Fracture conductivity (md-ft) | 100 |

**Table 3-4**: Reservoir and fracture parameters of the model

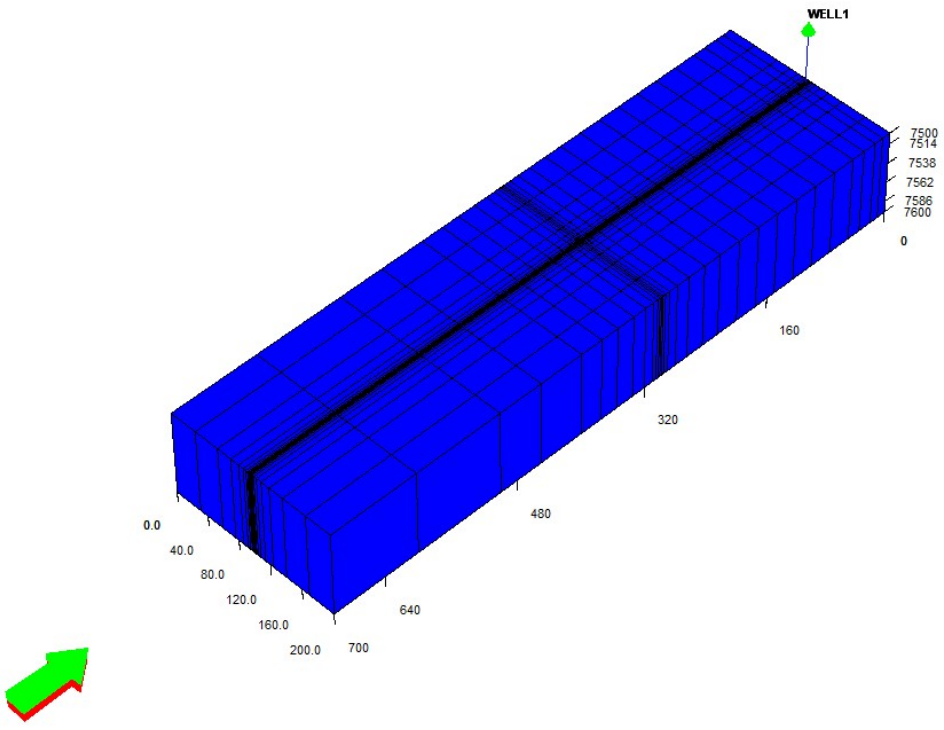


**Figure 3-5**: Simulation model for one segment

# Chapter 4: Results and Discussion

## 4.1 Mechanism

**Figure 4-1** shows the oil and gas cumulative production and production rate without treatment and with treatment using 100 mole/day/segment of DME at 200 days for rich gas condensate reservoir. **Figure 4-2** shows the oil and gas cumulative production and production rate without treatment and with treatment using 100 mole/day/segment of DME at 200 days for lean gas condensate reservoir. In the case with DME treatment, after 200 days of production, the well was shut in for 0.25 days. Then, DME was injected with a rate of 100 mole/day/segment (26.1 metric tons for whole well) for another 0.25 days. The well was kept shut in for 0.5 days after injection to let the reservoir soak. Finally, the producer was reopened until 600 days. The effectiveness of DME treatment for rich and lean gas condensate is significant as seen in the figures. After 600 days of production, for rich gas condensate, the cumulative oil production is increased by 19.71% after DME treatment and the cumulative gas production is increased by 68.41%. While for lean gas condensate, the cumulative oil production is increased by 16.41% after DME treatment and the cumulative gas production is increased by 63.42%, which is less obvious than that of rich gas condensate.

The mechanism of how condensate builds up along the fracture and obstructs gas production was demonstrated from rich gas condensate reservoir in **Figure 4-3**. As reservoir depleted, condensate saturation increased and accumulated especially along fractures. Gas saturation and gas relative permeability declined along fractures as condensate built up. The mechanism of removing the condensate from the fracture was described from rich gas condensate reservoir in **Figure 4-4**. The injected DME displaced both water and hydrocarbon components and completely swept the first few feet of the fracture right after injection. It can be observed that the removed condensate bank crept

back towards wellbore after 10 days of injection. DME treatment increased gas saturation and gas relative permeability adjacent to the wellbore from 0.52 to 0.70 and sustained even after 100 days of injection. It happened mainly because the pushed-back water near the wellbore remains immobile after injection as showed in **Figure 4-5**.

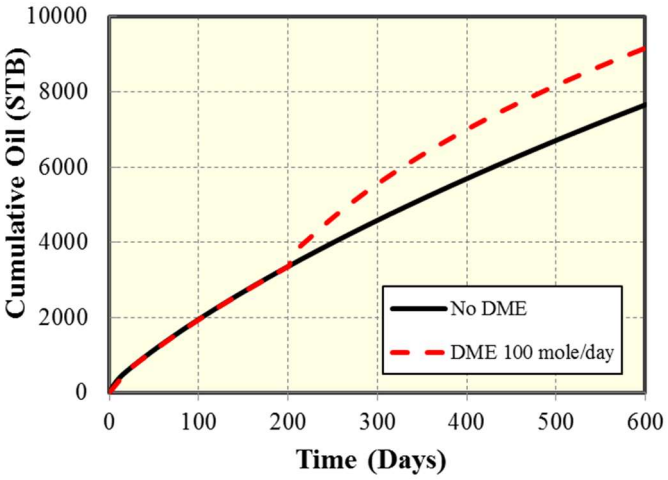


(a)

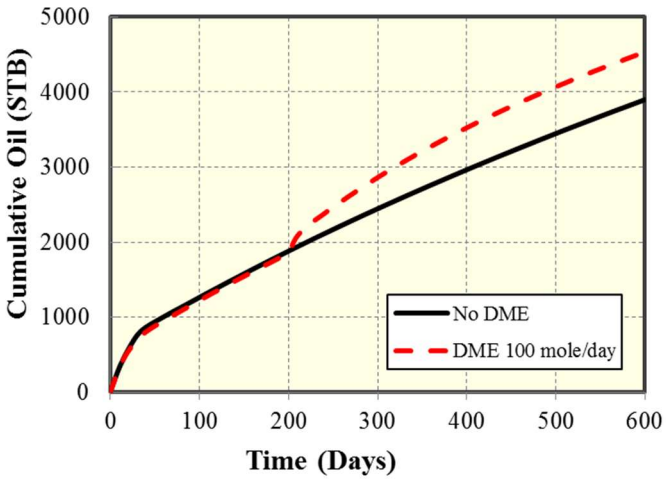


(a)

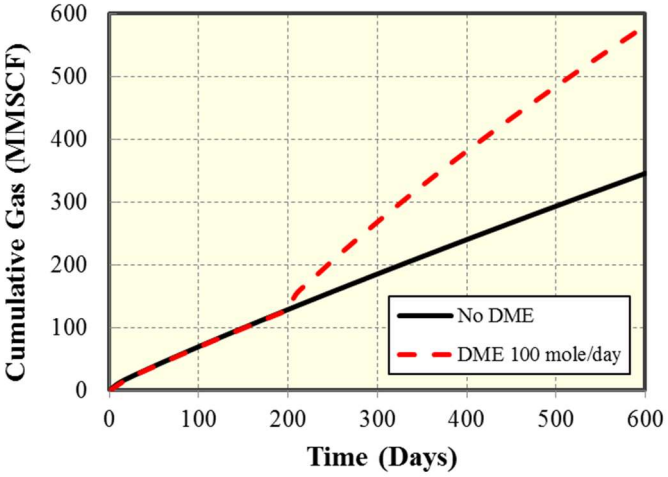


(b)

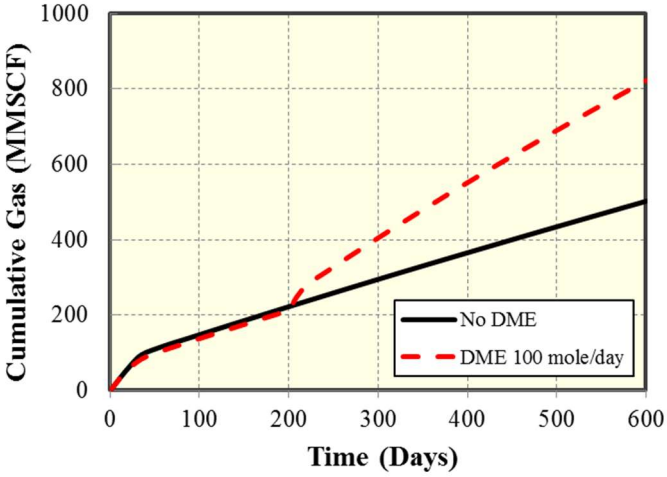


(b)

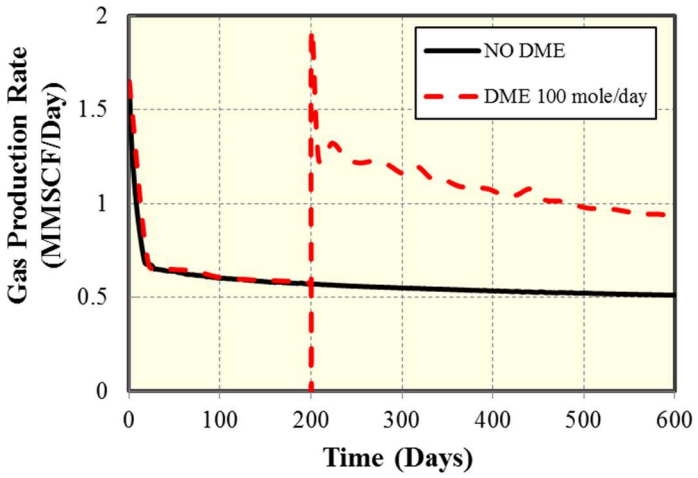


(c)

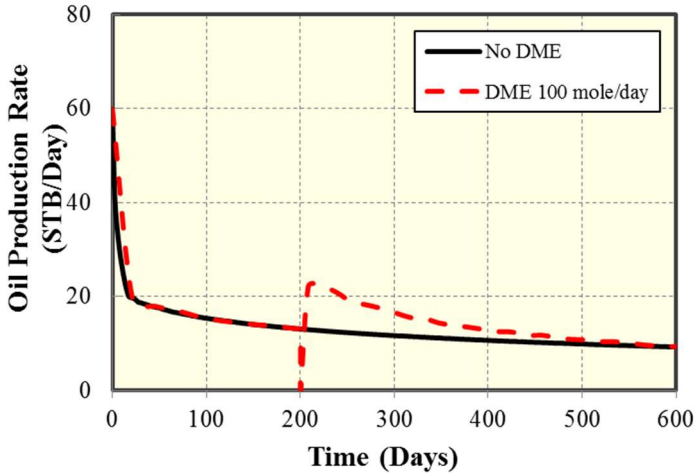


(d)

**Figure 4-1**: (a) Cumulative oil production (b) Cumulative gas production (c) Gas production rate (d) Oil production rate from rich gas condensate reservoir without treatment compared with DME 100 mole/day

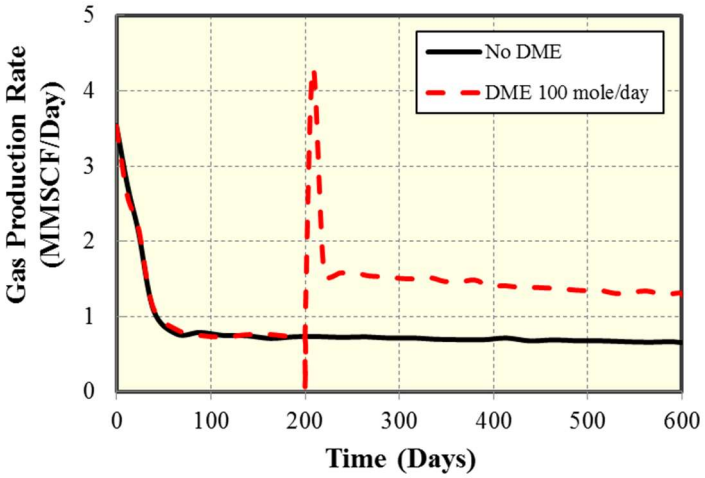


(c)

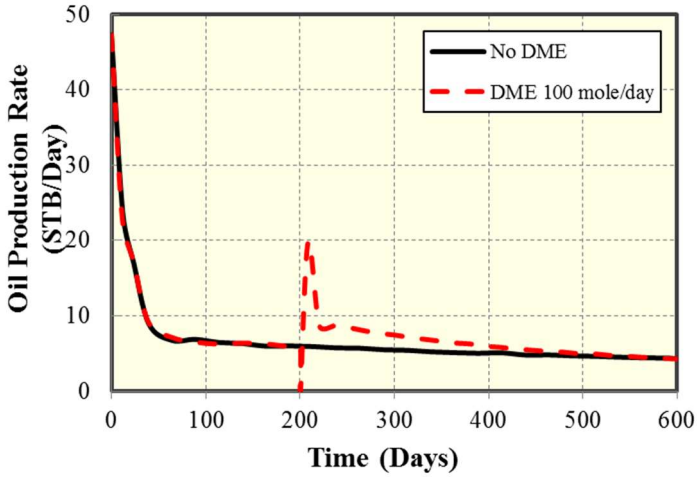


(d)

**Figure 4-2**: (a) Cumulative oil production (b) Cumulative gas production (c) Gas production rate (d) Oil production rate from lean gas condensate reservoir without treatment compared with DME 100 mole/day

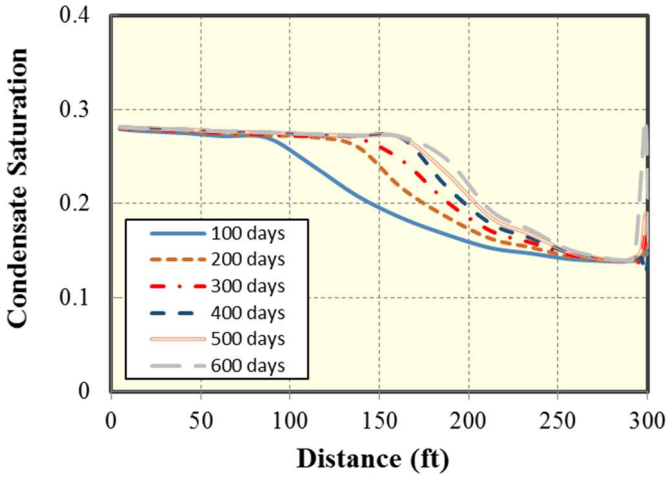
Condensate Saturation
0.4
0.3
0.2
0.1
0
100 days
200 days
300 days
400 days
500 days
600 days
0
50
100
150
200
250
300
Distance (ft)

(a)

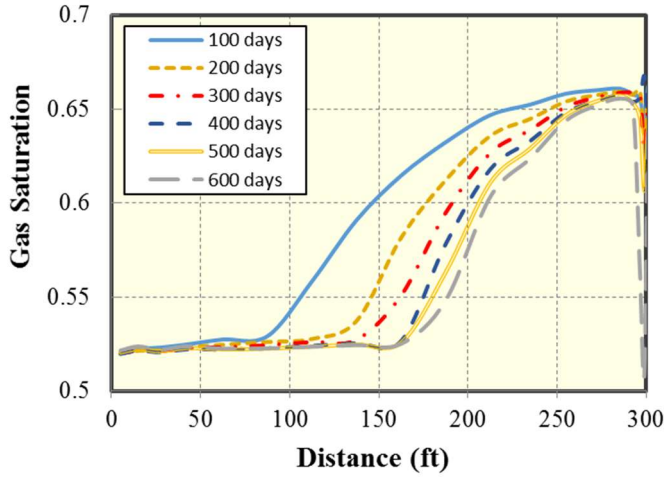
Gas Saturation
0.7
0.65
0.6
0.55
0.5
100 days
200 days
300 days
400 days
500 days
600 days
0
50
100
150
200
250
300
Distance (ft)

(b)

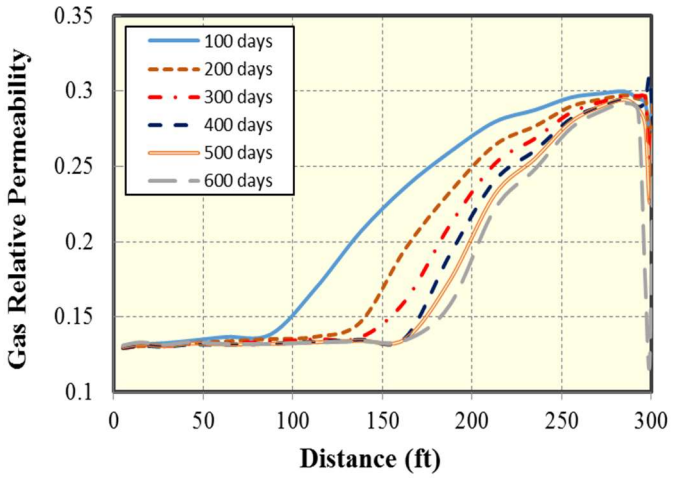


(c)

**Figure 4-3**: (a) Condensate buildup (b) Gas saturation (c) Gas relative permeability in fracture without treatment from rich gas condensate reservoir

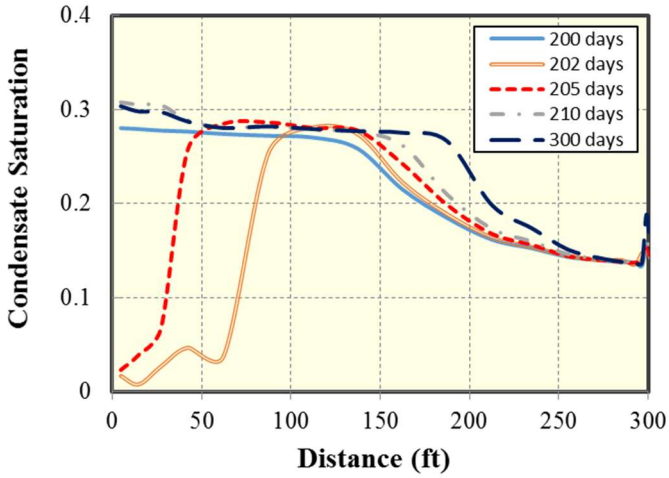


(a)

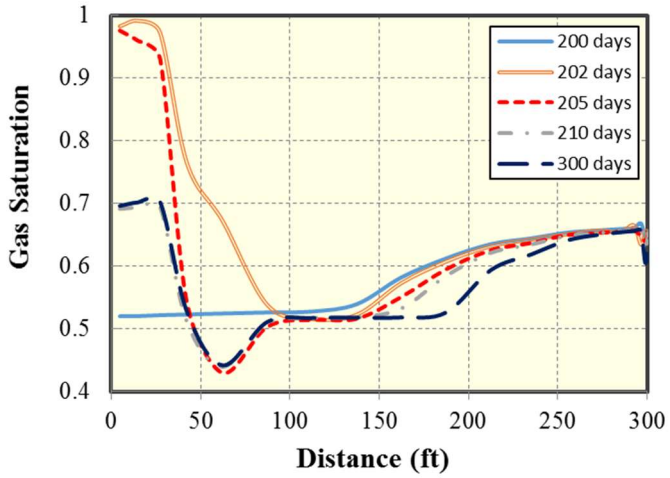


(b)

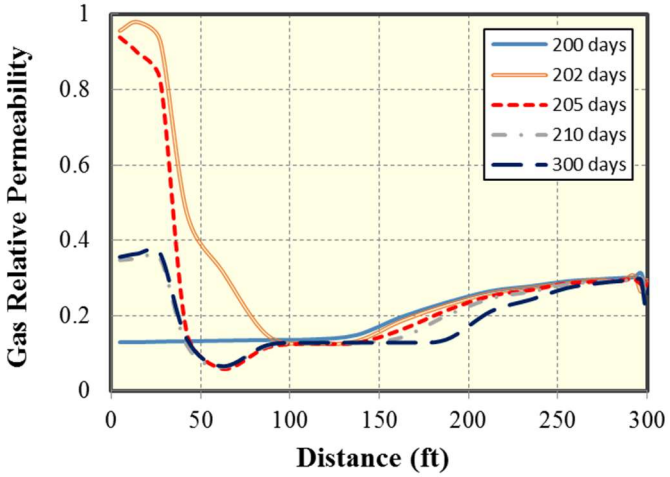


(c)

**Figure 4-4**: (a) Condensate buildup (b) Gas saturation (c) Gas relative permeability in fracture with DME injection 100 mole/day from rich gas condensate reservoir

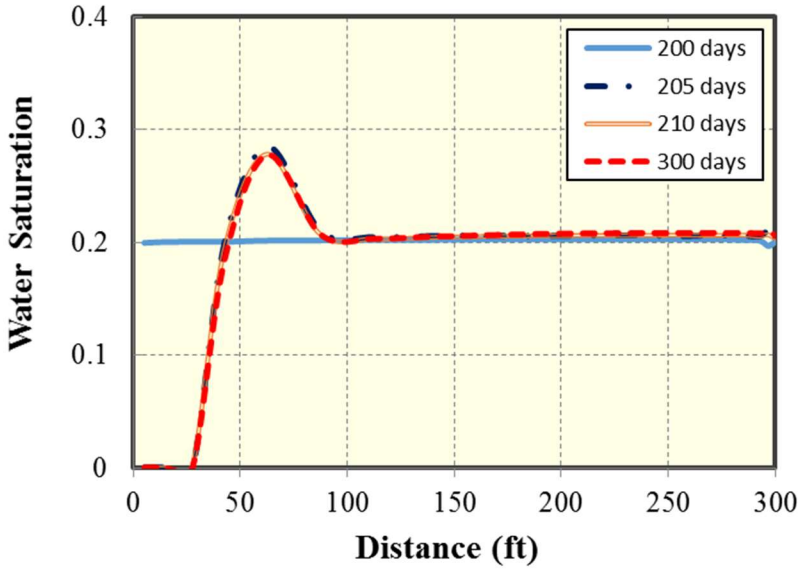


**Figure 4-5**: Water saturation in fracture with DME treatment 100 mole/day from rich gas condensate

From what has been discussed above, it is obvious that DME can effectively treat the solvent blockage. However, the pushed-back condensate would creep back toward wellbore only a few days after DME injection and gas relative permeability would also decay as production continuing. Hence, it is necessary to find the optimum injection patterns to make DME treatment economical.

## 4.2 Optimization variables

Now that the efficiency of DME treatment has been testified for both rich and lean gas condensate, next step is trying to find the variables which could possibly affect optimization of the treatment. The thesis investigated the impact from slug size, solvent mixture ratio and injection cycle.

### 4.1.1 Optimum Slug Size

The different slug sizes of the DME were compared with no DME treatment from rich gas condensate reservoir in **Figure 4-6**. Both 100 mole/day and 20 mole/day are more effective than 10 mole/day in improving cumulative oil and gas production and gas production rate. However, the impact of slug size is less obvious when the DME slug size increased from 20 mole/day to 100 mole/day. Also as slug size increases, the cost would become higher. Compared from the three slug size listed above, 20 mole/day/segment of DME could be regarded as an optimum value balancing the effectiveness and cost of treatment.

To investigate the reason why slug size above 20 mole/day would not make any difference on productivity, the condensate saturation, gas saturation and gas relative permeability with slug size of 10 mole/day and 20 mole/day was given in **Figures 4-7** and **4-8**. Comparing Figure 15 and 16 with Figure 12, it is obvious that more condensate along the fracture can be removed as slug size increasing. However, when the condensate within certain distance from the wellbore is removed, increasing slug size of DME would not make any difference on productivity.

To ascertain if the optimum slug size would be affected by reservoir properties, different slug sizes of DME were compared in the rich gas condensate reservoir with a permeability of 1000 nd and 162 nd. The results were shown in **Figures 4-9** and **4-10**. The cumulative oil and gas production is significantly decreased in the lower permeability reservoir before any treatment. The overall effectiveness of DME treatment is less obvious in the reservoir with permeability of 162 nd compared with that of 1000 nd. The cumulative oil production is almost the same before and after treatment with different slug sizes in the reservoir with permeability of 162 nd. The cumulative gas production and gas production rate in the reservoir with permeability of 162 nd still remain the trend found from that of 1000 nd, in which optimum slug size is 20 mole/day. The condensate saturation, gas

saturation and gas relative permeability in the reservoir k = 162 nd were shown in **Figure 4-11**. When the reservoir is much tighter, the liquid banking which can be removed by DME is much closer to the wellbore, which is not enough to improve oil recovery.

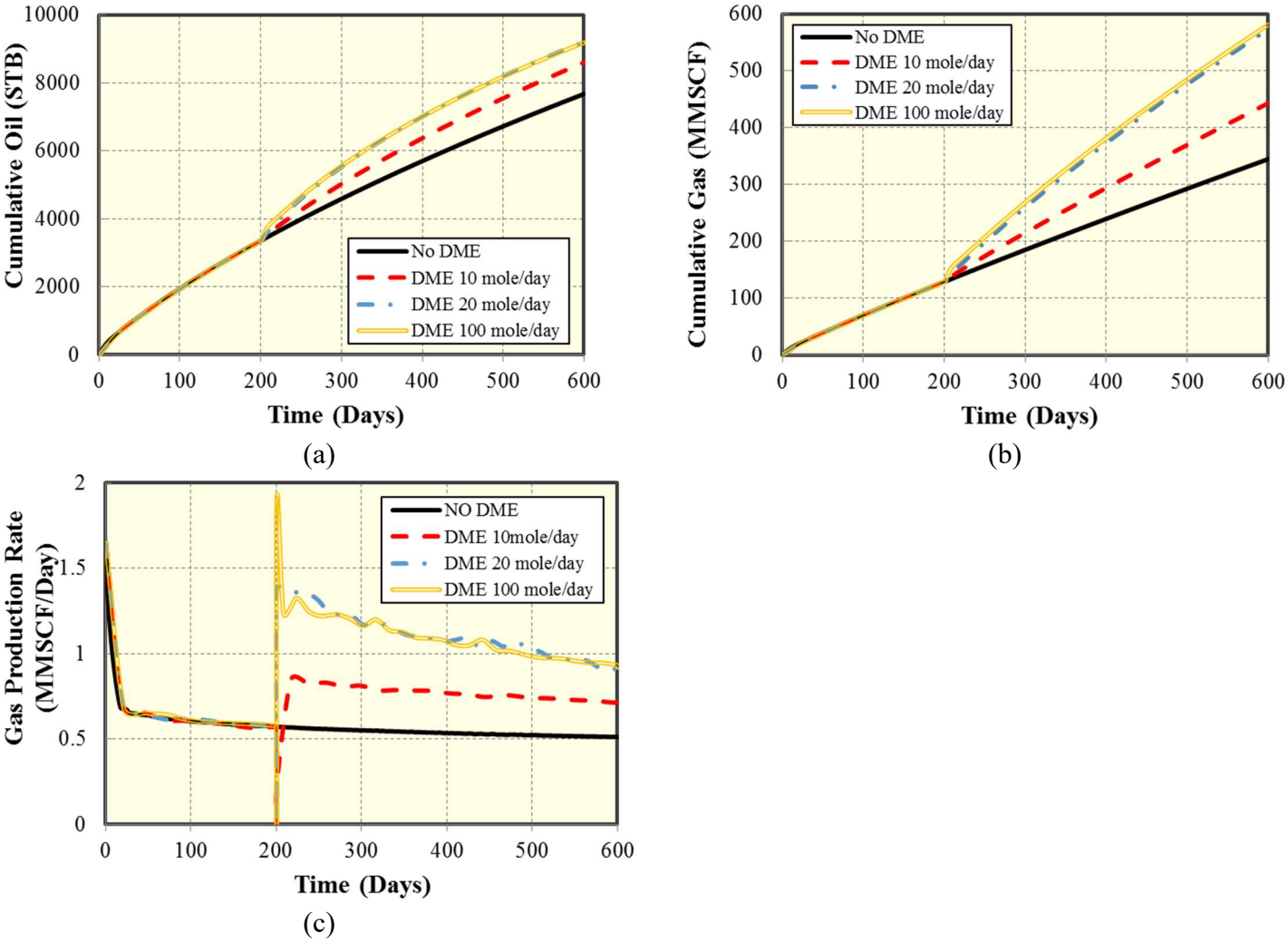


**Figure 4-6**: (a) Cumulative oil production (b) Cumulative gas production (c) Gas production rate from rich gas condensate reservoir without treatment compared with DME slug size of 10 mole/day, 20 mole/day and 100 mole/day

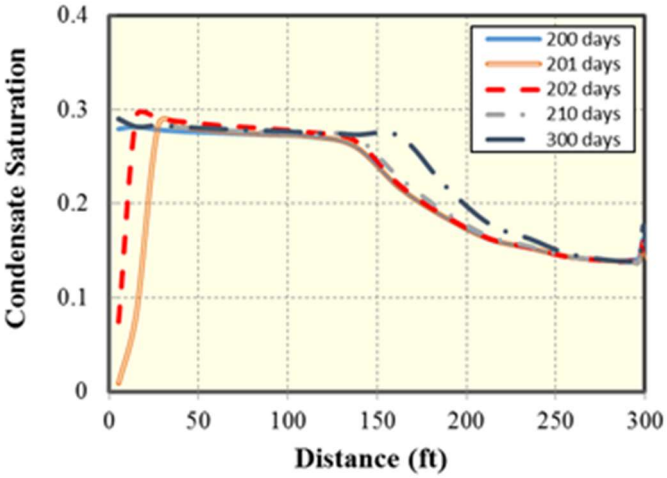
Condensate Saturation
Distance (ft)
200 days
201 days
202 days
210 days
300 days

(a)

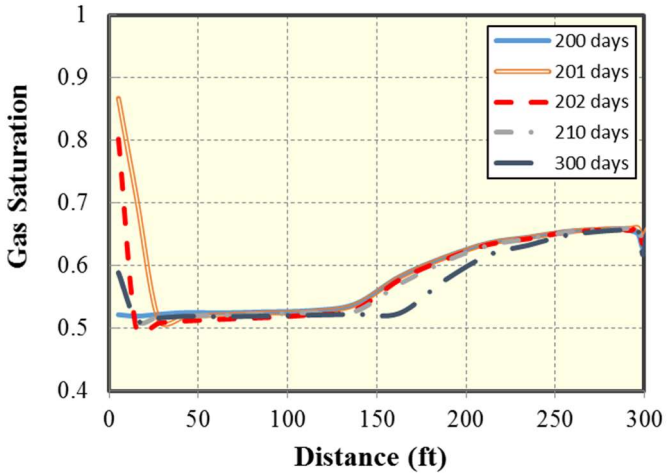
Gas Saturation
Distance (ft)
200 days
201 days
202 days
210 days
300 days

(b)

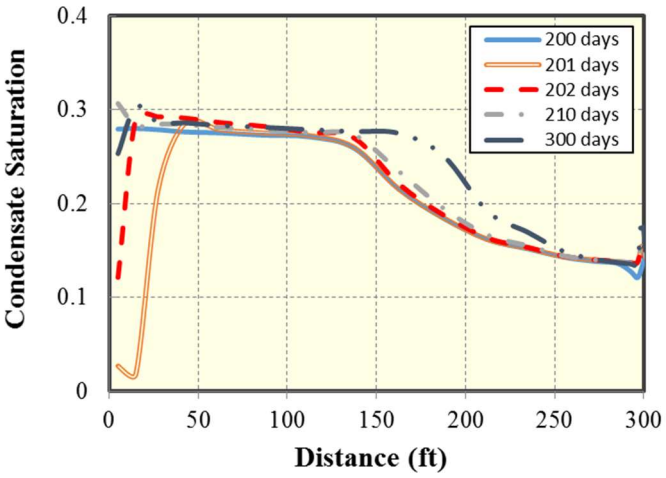
Condensate Saturation
Distance (ft)
200 days
201 days
202 days
210 days
300 days

(a)

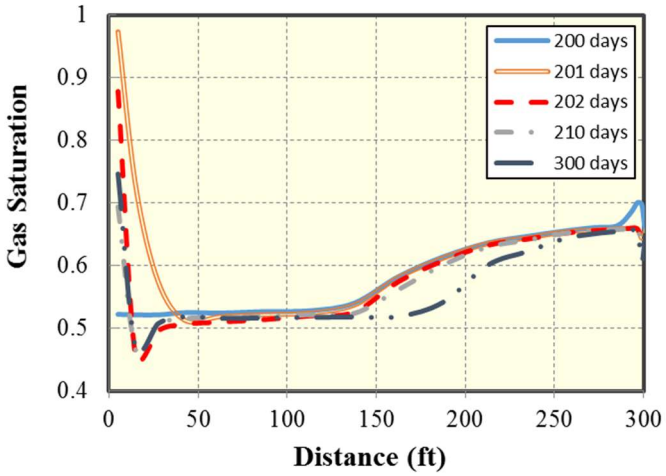
Gas Saturation
Distance (ft)
200 days
201 days
202 days
210 days
300 days

(b)

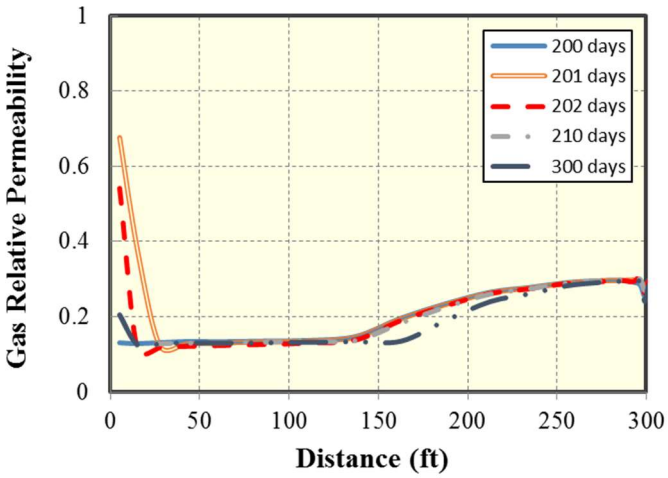


(c)

**Figure 4-7**: (a) Condensate buildup (b) Gas saturation (c) Gas relative permeability in fracture with DME injection 10 mole/day from rich gas condensate reservoir

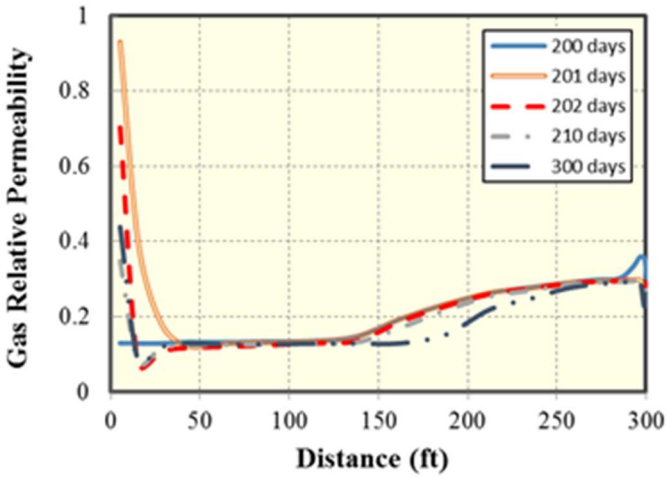


(c)

**Figure 4-8**: (a) Condensate buildup (b) Gas saturation (c) Gas relative permeability in fracture with DME injection 20 mole/day from rich gas condensate reservoir

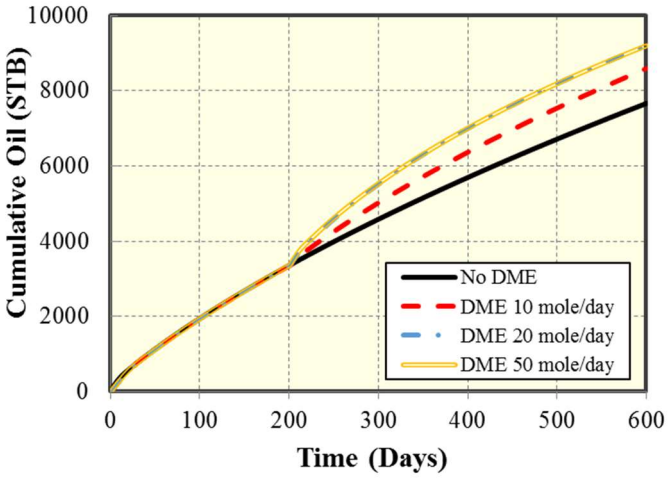


(a)

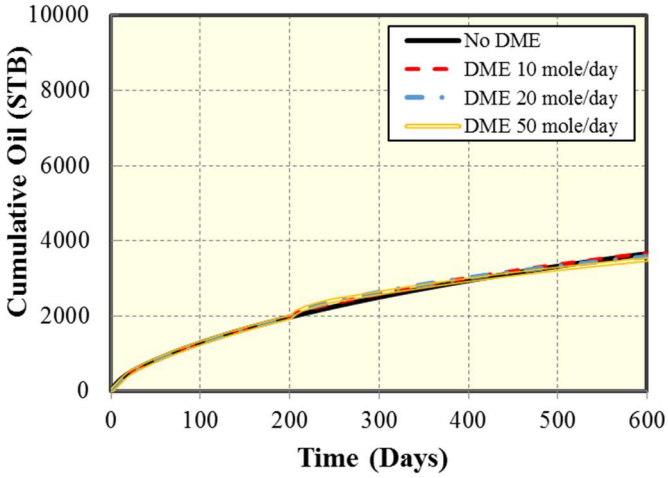


(a)

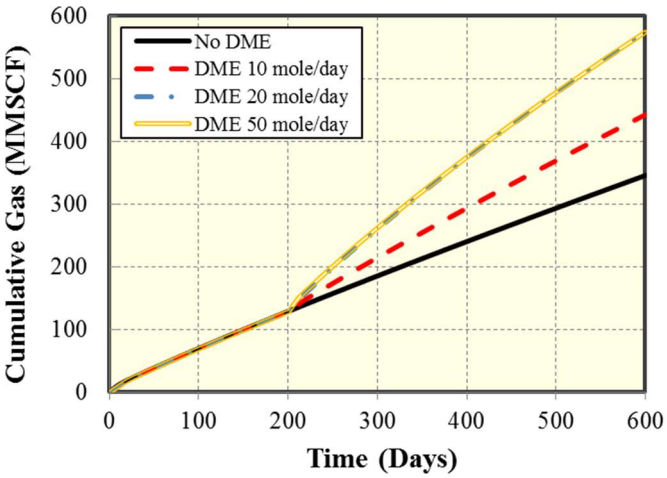


(b)

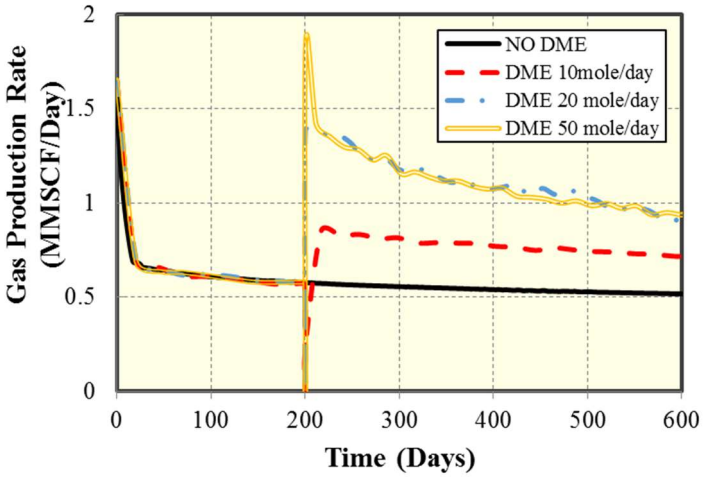


(c)

**Figure 4-9**: (a) Cumulative oil production (b) Cumulative gas production (c) Gas production rate from rich gas condensate reservoir with permeability of 1000 nd without treatment compared with DME slug size of 10 mole/day, 20 mole/day and 50 mole/day

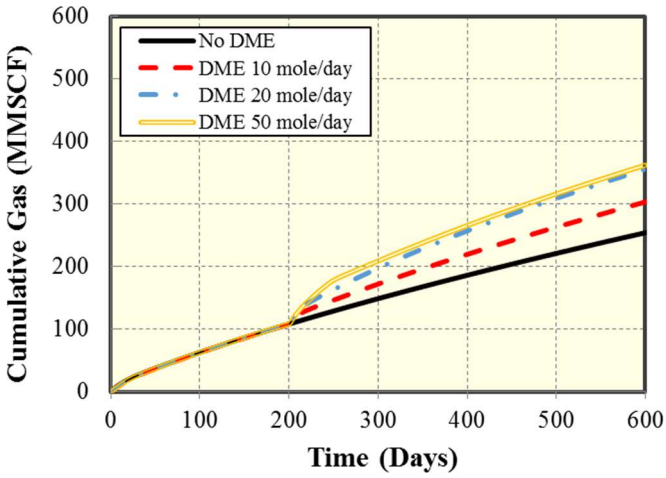


(b)

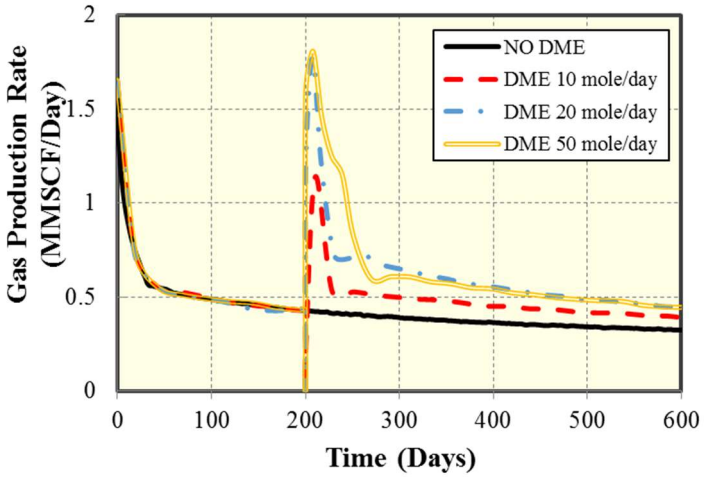


(c)

**Figure 4-10**: (a) Cumulative oil production (b) Cumulative gas production (c) Gas production rate from rich gas condensate reservoir with permeability of 162 nd without treatment compared with DME slug size of 10 mole/day, 20 mole/day and 50 mole/day

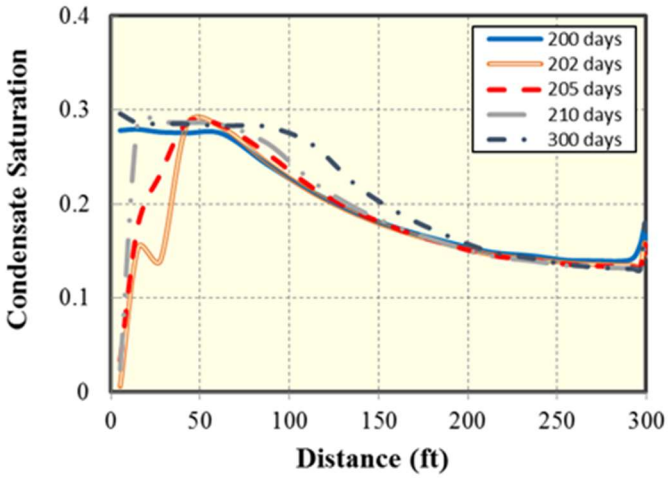
Condensate Saturation
0.4
0.3
0.2
0.1
0
0
50
100
150
200
250
300
Distance (ft)
200 days
202 days
205 days
210 days
300 days

(a)

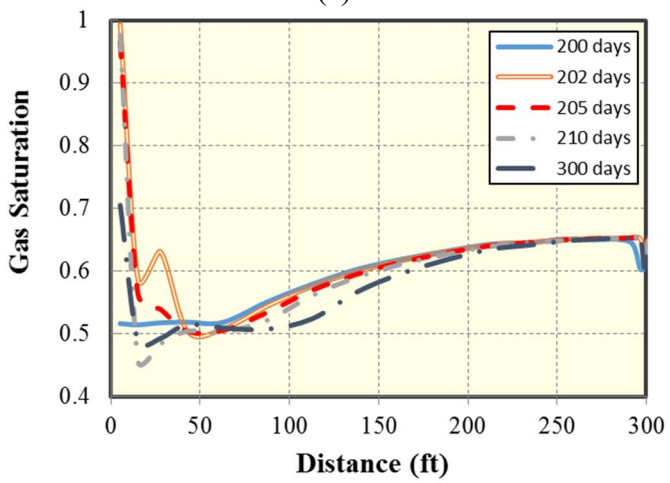
Gas Saturation
1
0.9
0.8
0.7
0.6
0.5
0.4
0
50
100
150
200
250
300
Distance (ft)
200 days
202 days
205 days
210 days
300 days

(b)

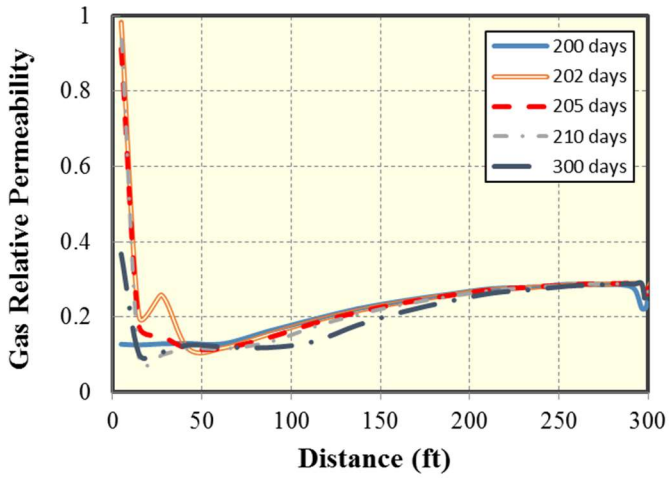


(c)

**Figure 4-11**: (a) Condensate buildup (b) Gas saturation (c) Gas relative permeability in fracture with DME injection 20 mole/day from rich gas condensate reservoir k=162nd

### 4.1.2 Optimum Solvent Mixture

It is possible that mixing DME with cheaper gas slug like $N_2$ to lower the cost but maintain the same efficiency as pure DME. Since the performance of treatment could be significantly different below and above 20 mole/day, it is necessary to test the behavior of the mixture with different slug sizes. The different slug sizes of DME were mixed with 20% of $N_2$ and results were compared in **Figures 4-12 and 4-13**. When 20% of $N_2$ was mixed with treatment using a total 10 mole/day/segment of DME+$N_2$, the cumulative oil and gas production and gas production rate were weakened significantly compared with only 10 mole/day/segment of DME. However, in the scenario with the slug size of 20 mole/day, 20% of $N_2$ mixture only slightly impaired the cumulative gas production while cumulative oil production and gas production rate almost remained the same compared

with that of pure DME. Since the DME mixture with 20% of $N_2$ would consume less DME, it is an economical way to inject with 20% of $N_2$ mixture instead when the treatment effectiveness is not obviously weakened.

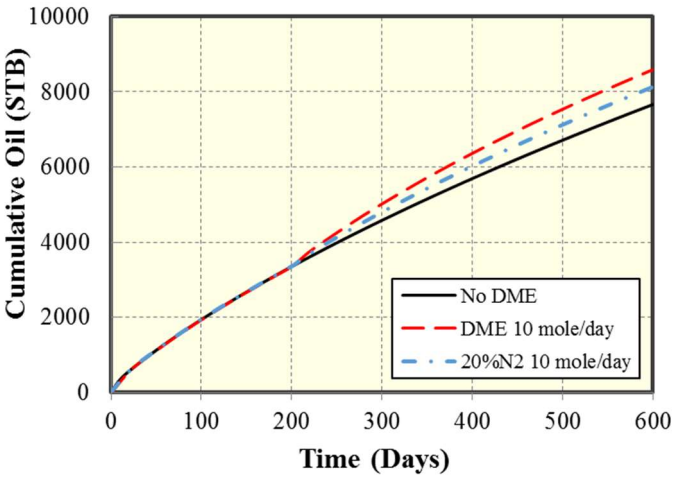


(a)

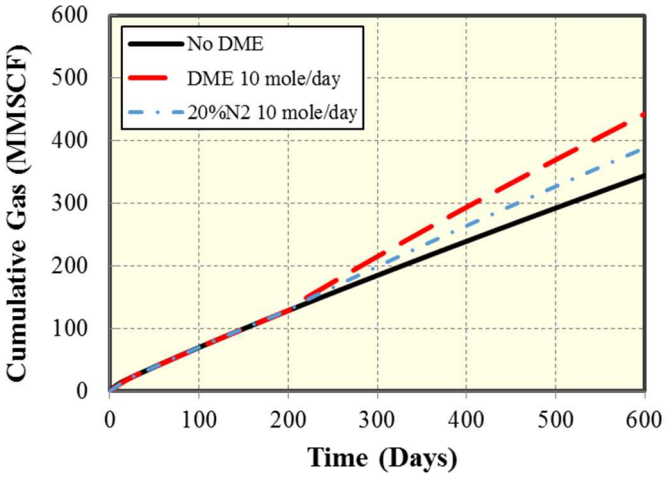


(b)

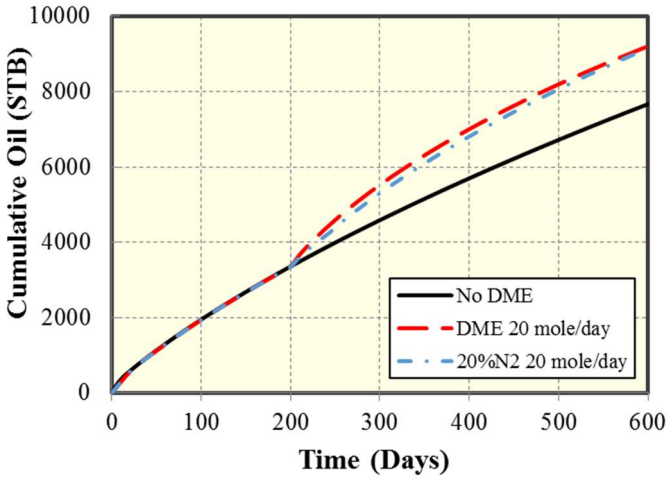


(a)

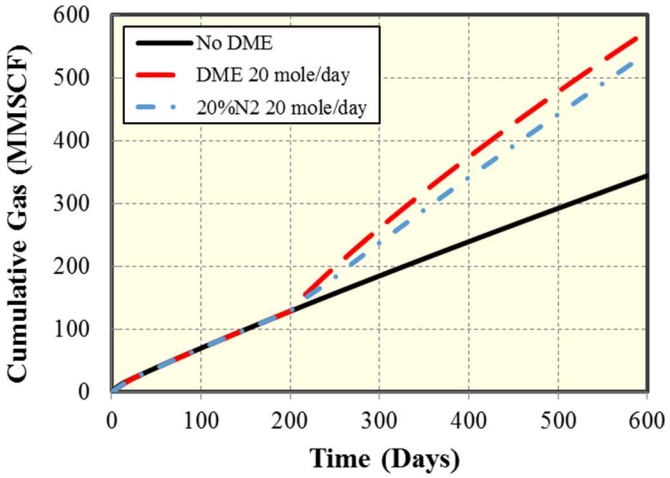


(b)

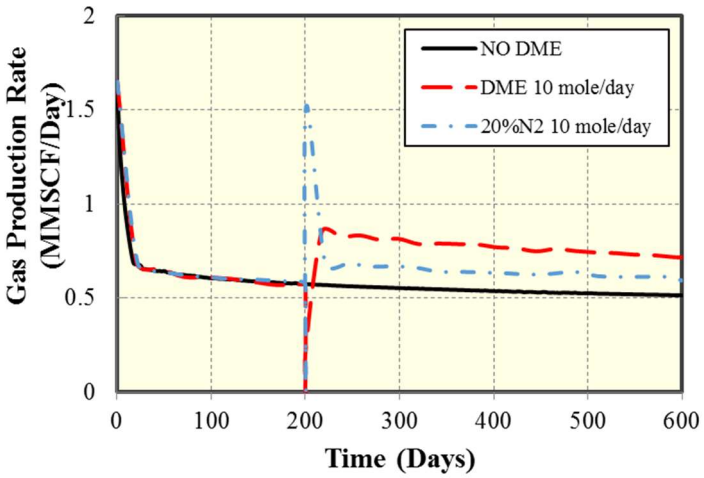


(c)

**Figure 4-12**: (a) Cumulative oil production (b) Cumulative gas production (c) Gas production rate from rich gas condensate reservoir without treatment compared with 10 mole/day/segment of DME and 10 mole/day/segment of DME mixed with 20% of $N_2$

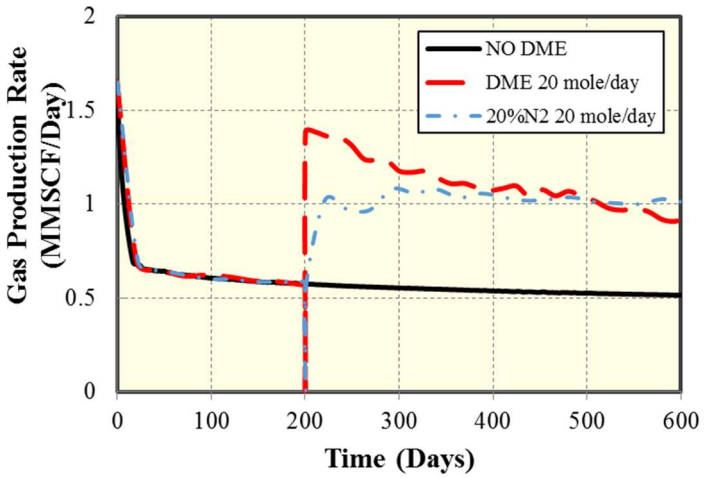


(c)

**Figure 4-13**: (a) Cumulative oil production (b) Cumulative gas production (c) Gas production rate from rich gas condensate reservoir without treatment compared with 20 mole/day/segment of DME and 20 mole/day/segment of DME mixed with 20% of $N_2$

### 4.1.3 Optimum Cycle of Injection

Considering the pushed back condensate would creep back and block fractures a few days after injection, sometimes it is necessary to repeat injecting DME. Hence, different injection cycles with varying slug sizes of DME treatment were compared to evaluate the effectiveness. **Figures 4-14 and 4-15** show the cumulative oil and gas production and gas production rate with 10 mole/day/segment injected twice at 150 days and 250 days and 150 days and 350 days. **Figures 4-16 and 4-17** show the cumulative oil and gas production and gas production rate with 20 mole/day/segment injected twice at 150 days and 250 days and 150 days and 350 days. In all cases, the cumulative oil production was not affected by different injection cycle. But with slug size of 10 mole/day,

the cumulative gas production could be different in the two injection cycles. To further investigate the influence of reinjection on gas production, **Figure 4-18** shows the cumulative gas production with DME reinjected at different period with 10 mole/day and compares the results with slug size of 20 mole/day one-time treatment. Reinjection at early period with 10 mole/day (150 and 200 days or 150 and 250 days) has the same effectiveness with that of 20 mole/day one-time treatment, while reinjection at the late production period would be less effective.

Although the different injection cycles did not impact much on the oil production, the productivity is sensitive to different slug sizes in the same injection cycle. With 10 mole/day/segment first injected at 150 days, reinjecting at 250 or 350 days would both significantly improve cumulative oil and gas production and gas production rate. However, with 20 mole/day treatment twice, only cumulative gas production was improved slightly more than that of treatment once. Cumulative produced oil and gas production at 600 days remains the same with injected DME once.

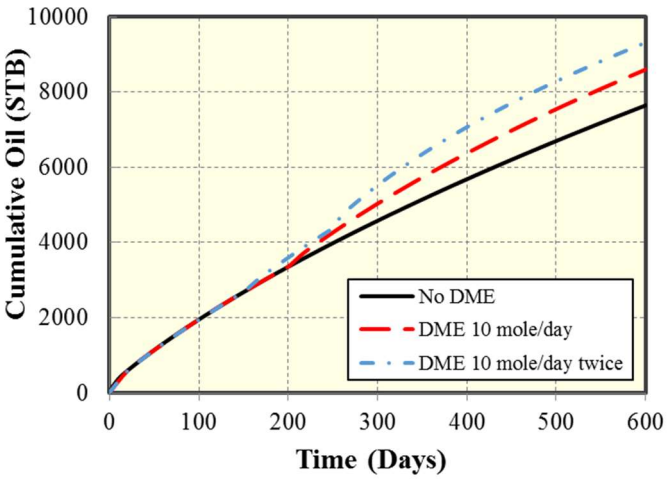

(a)

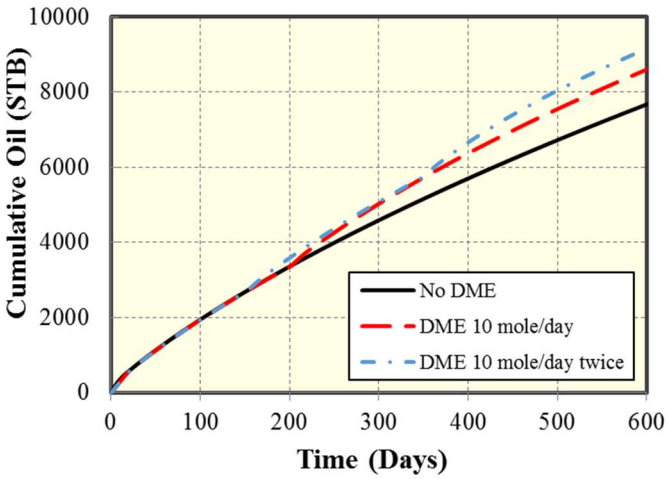

(a)

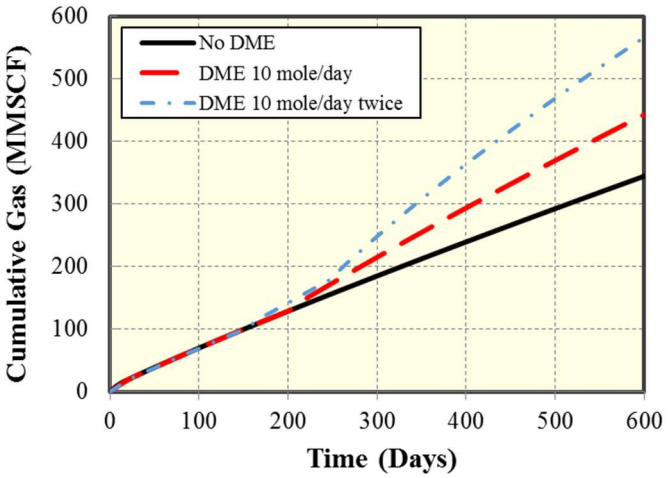


(b)

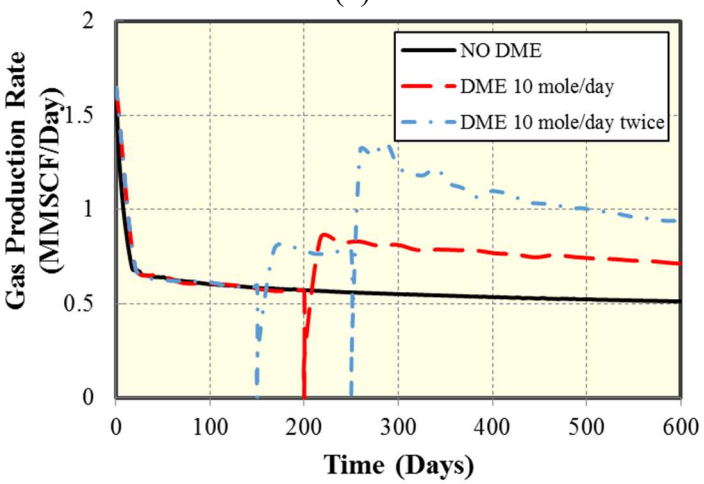


(c)

**Figure 4-14**: (a) Cumulative oil production (b) Cumulative gas production (c) Gas production rate from rich gas condensate reservoir without treatment compared with 10 mole/day injected once at 200 days and injected twice at 150 and 250 days

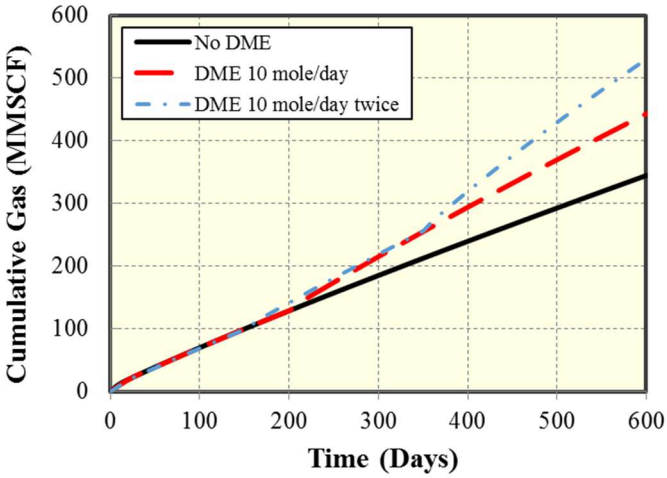


(b)

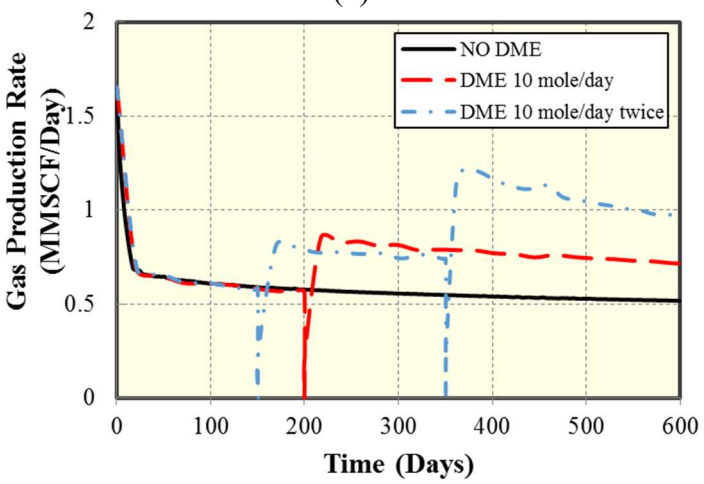


(c)

**Figure 4-15**: (a) Cumulative oil production (b) Cumulative gas production (c) Gas production rate from rich gas condensate reservoir without treatment compared with 10 mole/day injected once at 200 days and injected twice at 150 and 350 days

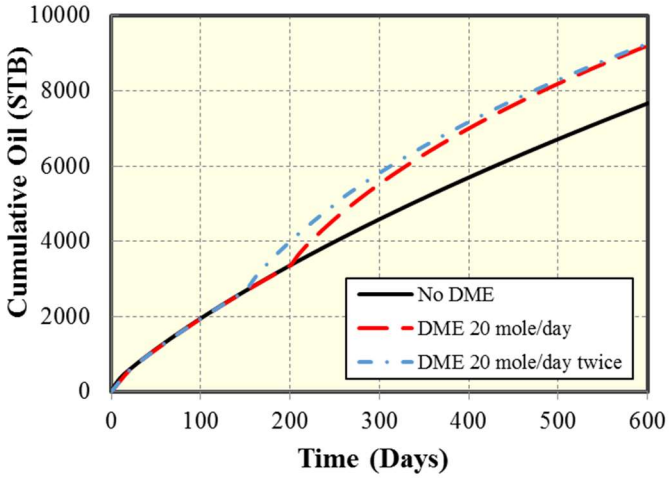
Cumulative Oil (STB)
10000
8000
6000
4000
2000
0
0
100
200
300
400
500
600
Time (Days)
No DME
DME 20 mole/day
DME 20 mole/day twice

(a)

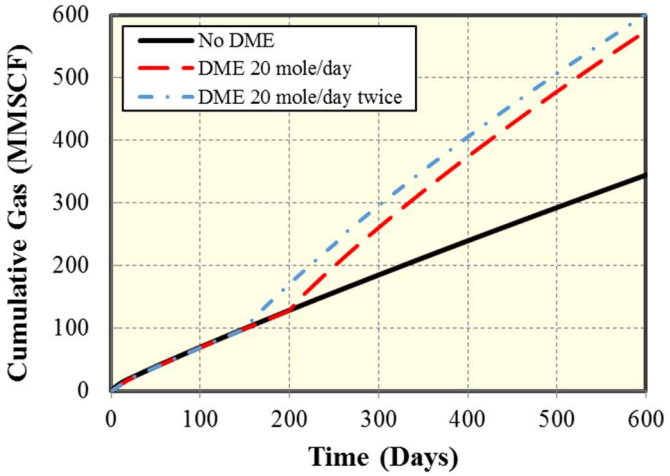
Cumulative Gas (MMSCF)
600
500
400
300
200
100
0
0
100
200
300
400
500
600
Time (Days)
No DME
DME 20 mole/day
DME 20 mole/day twice

(b)

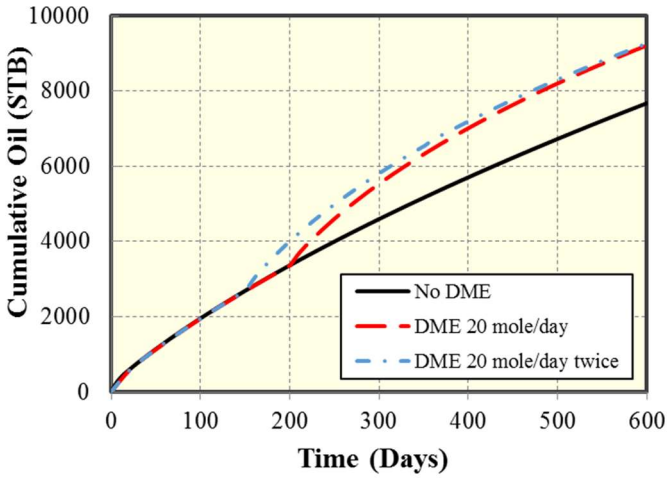
Cumulative Oil (STB)
10000
8000
6000
4000
2000
0
0
100
200
300
400
500
600
Time (Days)
No DME
DME 20 mole/day
DME 20 mole/day twice

(a)

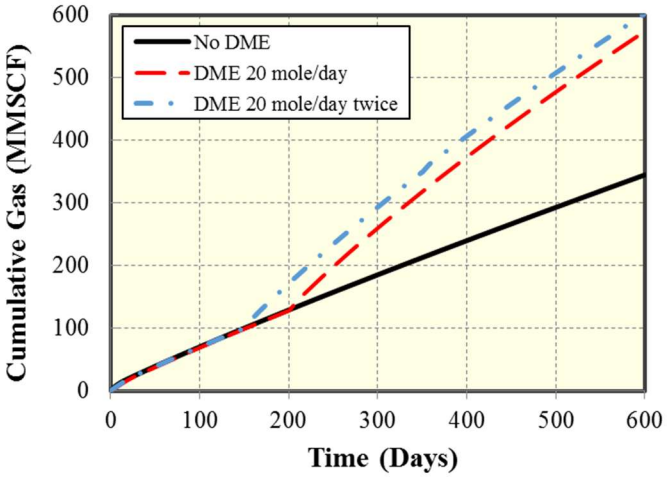
Cumulative Gas (MMSCF)
600
500
400
300
200
100
0
0
100
200
300
400
500
600
Time (Days)
No DME
DME 20 mole/day
DME 20 mole/day twice

(b)

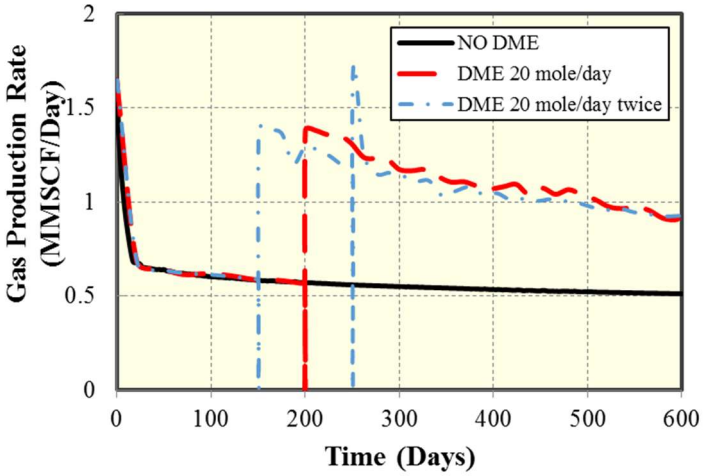


(c)

**Figure 4-16**: (a) Cumulative oil production (b) Cumulative gas production (c) Gas production rate from rich gas condensate reservoir without treatment compared with 20 mole/day injected once at 200 days and injected twice at 150 and 250 days

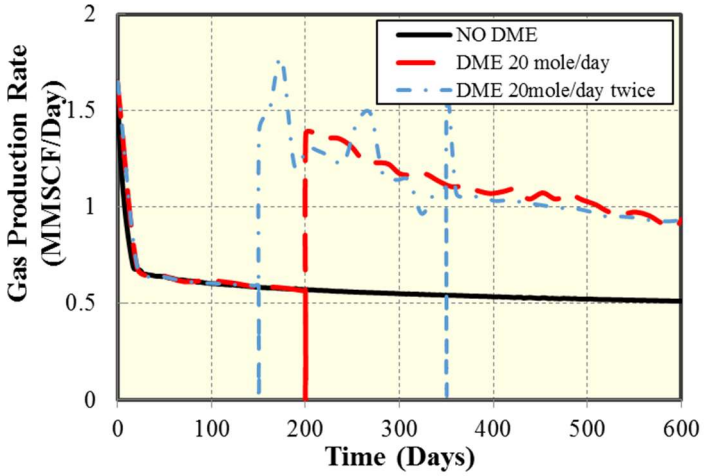


(c)

**Figure 4-17**: (a) Cumulative oil production (b) Cumulative gas production (c) Gas production rate from rich gas condensate reservoir without treatment compared with 20 mole/day injected once at 200 days and injected twice at 150 and 350 days

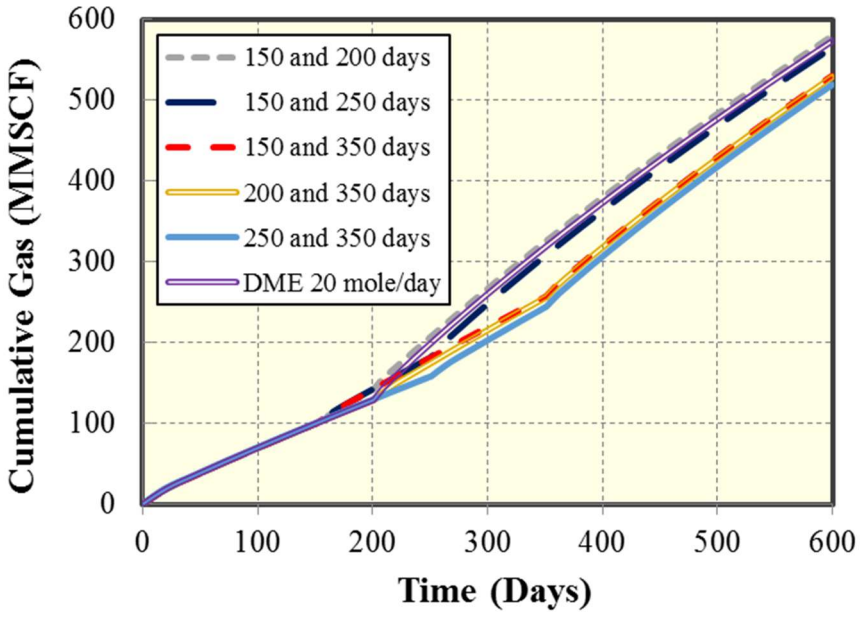

**Figure 4-18**: Cumulative gas production of different reinjection cycle with slug size of 10 mole/day compared with DME treatment once 20 mole/day

### 4.3 Net present value

From previous discussion, there is a critical slug size for the rich gas condensate fluid in this study that below or above this value the performance of solvent mixture ratio and reinjection would be different. Also, for the same amount of DME, it is more effective when DME is injected one-time at the early stage of production. Therefore, this section mainly discusses the economic impact caused by different amount of DME for one-time injection. Net present value (NPV) is proposed as the objective function to further quantify the economic effect from the critical slug size and DME ratio. In this study, the NPV was defined as the difference from the revenue minus the investment. The price for oil, gas and DME used for the NPV model was listed in **Table 4-1**. The oil and gas price were estimated from the recent price trend and the DME price was obtained from market outlook for dimethyl ether (2002). The cost of $N_2$ was neglected.

Due to the low dimensions of this optimization problem, which only two variables were included to evaluate NPV, the brute force search (exhaustive search) was used to enumerate all the possible combination. The range and step for two variables were listed in **Tables 4-2 and 4-3**. The results of NPV distribution were shown in **Figures 4-19 and 4-20**.

| | |
|---|---|
| Oil price ($/STB) | 70 |
| Gas price ($/MSCF) | 5 |
| DME price ($/lb) | 3 |

**Table 4-1**: Parameters for the NPV calculation

| | Slug size (mole/day) | DME ratio |
|---|---|---|
| k = 1000 nd | 5 - 50 | 0.5 – 0.92 |
| k = 500 nd | 5 - 50 | 0.5 - 1 |
| k = 100 nd | 5 - 80 | 0.5 - 1 |

**Table 4-2**: The range of variables at different reservoir permeabilities

| | Slug size (mole/day) | DME ratio |
|---|---|---|
| k = 1000 nd | 3 | 0.02 |
| k = 500 nd | 3 | 0.02 |
| k = 100 nd | 5 | 0.05 |

**Table 4-3**: The step of variables at different reservoir permeabilities

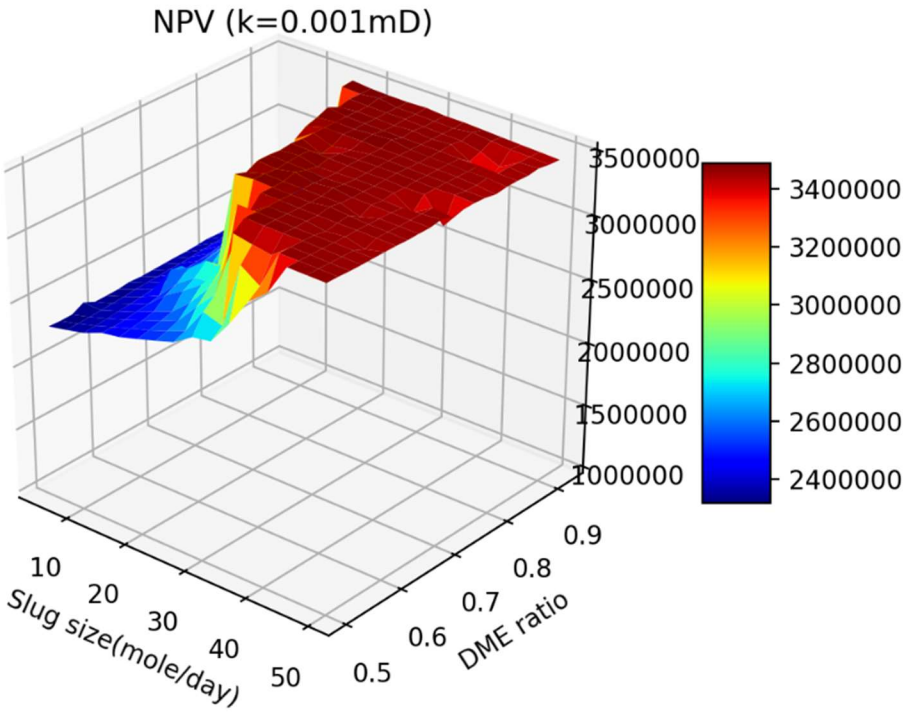
NPV (k=0.001mD)
3500000
3000000
2500000
2000000
1500000
1000000
3400000
3200000
3000000
2800000
2600000
2400000
10
20
30
40
50
Slug size(mole/day)
0.5
0.6
0.7
0.8
0.9
DME ratio

(a)

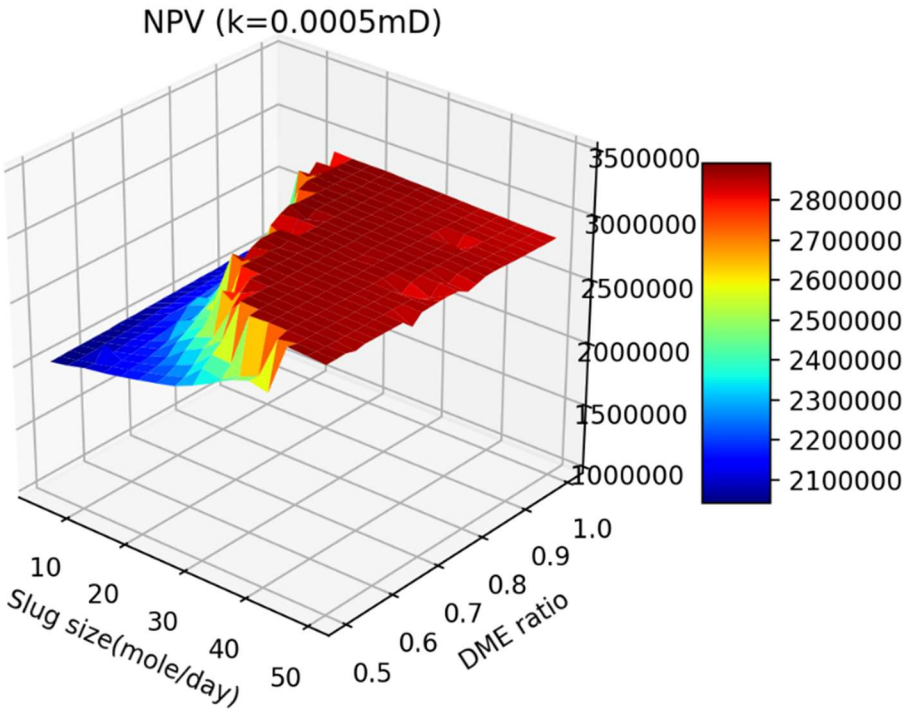
NPV (k=0.0005mD)
3500000
3000000
2500000
2000000
1500000
1000000
2800000
2700000
2600000
2500000
2400000
2300000
2200000
2100000
10
20
30
40
50
Slug size(mole/day)
0.5
0.6
0.7
0.8
0.9
1.0
DME ratio

(b)

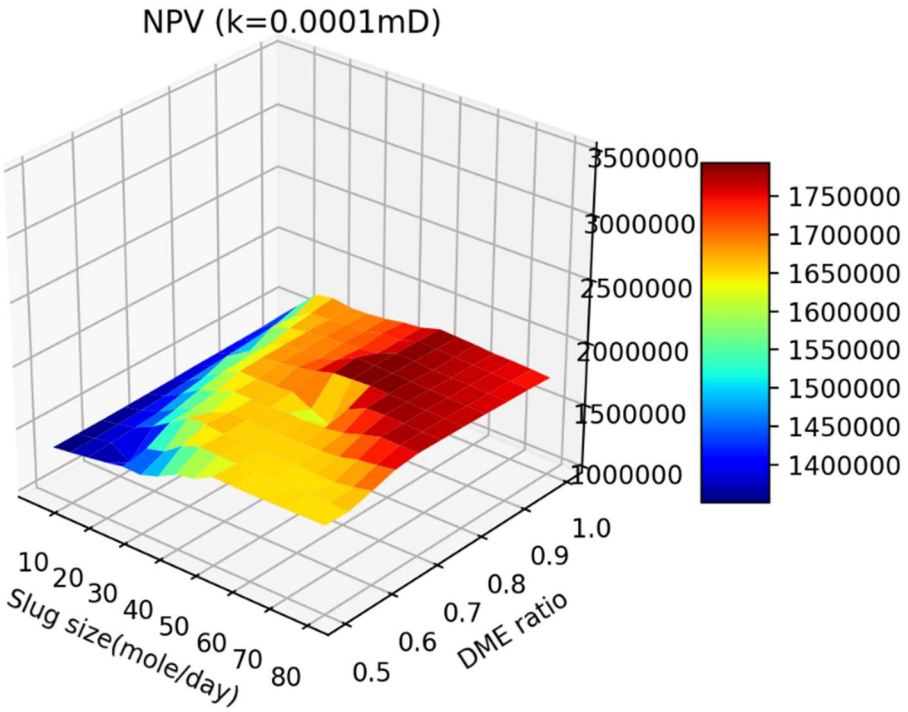


(c)

**Figure 4-19**: NPV surface plot from reservoir with permeability (a) k = 1000 nd (b) k = 500 nd (c) k = 100 nd

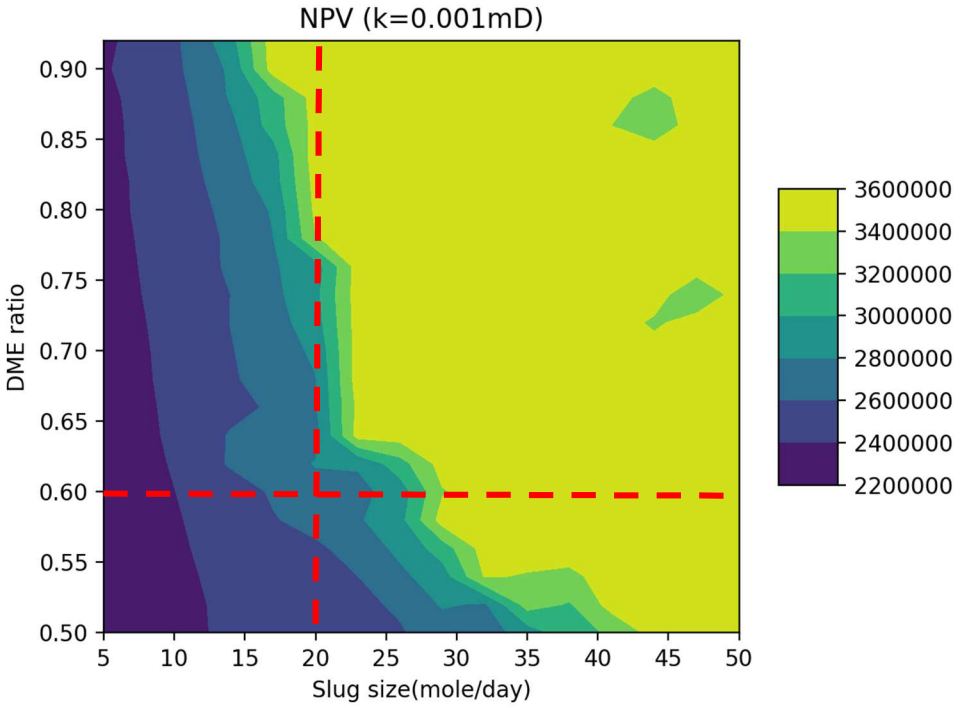
NPV (k=0.001mD)
DME ratio
0.90
0.85
0.80
0.75
0.70
0.65
0.60
0.55
0.50
5
10
15
20
25
30
35
40
45
50
Slug size(mole/day)
3600000
3400000
3200000
3000000
2800000
2600000
2400000
2200000

(a)

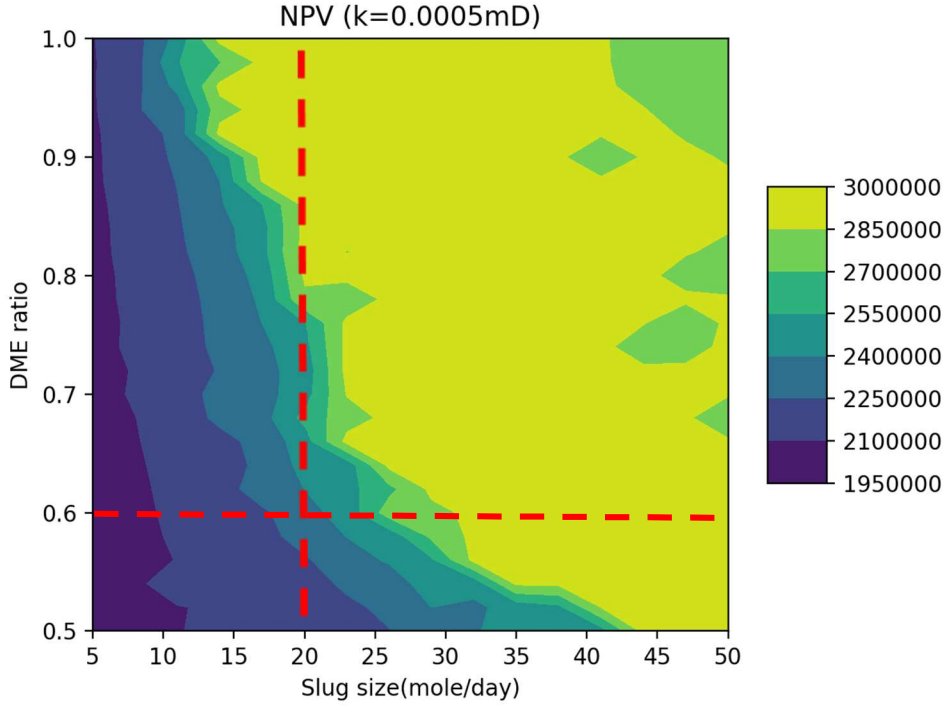
NPV (k=0.0005mD)
DME ratio
1.0
0.9
0.8
0.7
0.6
0.5
5
10
15
20
25
30
35
40
45
50
Slug size(mole/day)
3000000
2850000
2700000
2550000
2400000
2250000
2100000
1950000

(b)

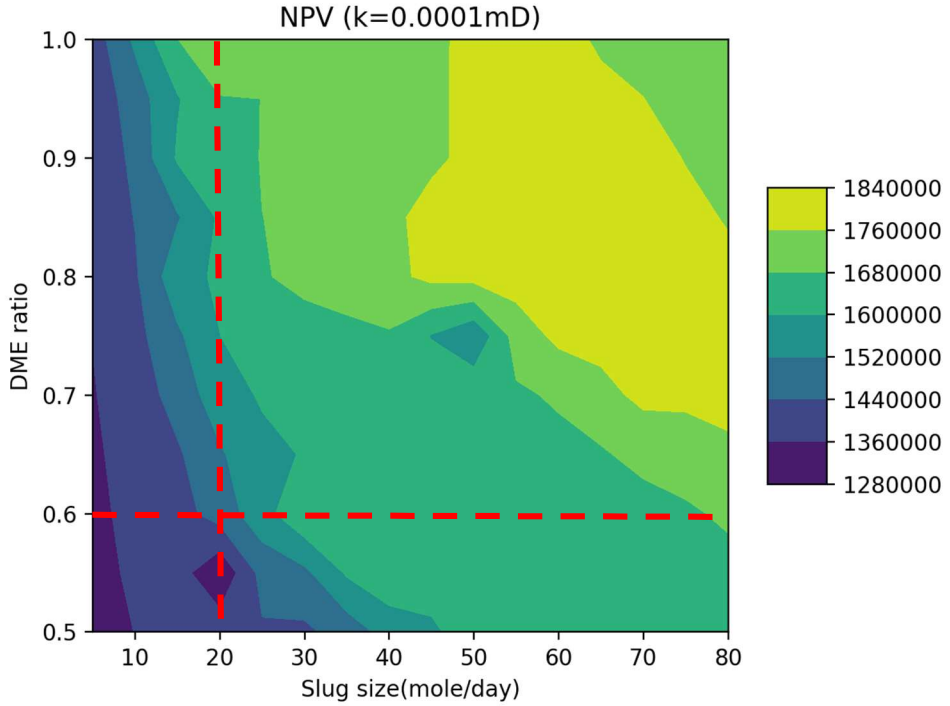


(c)

**Figure 4-20**: NPV contour plot from reservoir with permeability (a) k = 1000 nd (b) k = 500 nd (c) k = 100 nd

As the reservoir permeability decreases, the overall NPV decreases significantly. The vertical dot line on the contour plots points out the slug size of 20 mole/day (see Figure 4-20). At each given reservoir permeability, it is obvious that NPV increases sharply when slug size is below 20 mole/day (left side of the line). While the slug size is above 20 mole/day (right side of the line), NPV increases slowly or almost remains constant. The above observation sustains until the DME ratio is below 0.6.

The NPV on right side of the vertical dot line is roughly 90% of the highest NPV on each contour plot. While the DME ratio is above 0.6, slug size is the key factor in NPV

analysis. Therefore, 20 mole/day can be regarded as a critical value if 90% of the highest NPV is taken as the cutoff point. Once DME ratio is less than 0.6, both ratio and slug size would affect NPV.

# Chapter 5: Conclusions

## 5.1 Conclusions

The compositional simulator UTCOMP with a robust three phase flash calculation option is capable of capturing the phase behavior of the solvent/hydrocarbons/water mixture. Condensate buildup would significantly reduce the production rate by decreasing the gas relative permeability. In the study, it is shown that DME treatment is capable of improving the productivity of both rich and lean fractured shale gas condensate reservoir by removing the liquid blocks along the fracture. Also, the efficiency of DME can be sustained at the range of permeability from the magnitude of 100 nd to 1000 nd. But DME treatment is more effective for gas production than oil production when the reservoir permeability is around 100 nd. It would happen mainly because DME treatment cannot go further from the wellbore to improve oil production. Considering the cost and decay of the treatment during production, more simulations are needed to find the optimum way for DME treatment.

According to the simulation results in this study, there exists a critical slug size for DME, below or above which the performance of treatment would be significantly different. The main reason is that once all the liquid near the wellbore has been removed, the liquid further from the wellbore would not affect productivity. The critical value remains the same for the same fluid model but different permeabilities. For the rich gas condensate fluid in the study, 20 mole/day/segment of DME is a critical slug size. Below the slug size of 20 mole/day/segment, the effectiveness would be affected by different slug sizes, the composition of $N_2$ mixture and reinjection times. While reinjection times would influence the production with slug size below critical value, the cycle of reinjection would not affect oil production. For the same amount of DME, the treatment is more effective on gas when starting treatment at the early period of production with slug size below 20 mole/day.

However, when the slug size is above 20 mole/day, the impact from solvent mixture on production would also be weakened. Hence, it could possibly be more economical to use the slug size with cheaper solvent mixture instead of pure DME to reach the same treatment effectiveness.

To further investigate the economic impact of DME for one-time injection, NPV was proposed to quantify the revenue and investment during the production. NPV at different permeabilites was compared. When reservoir formation is tighter, the revenue is less, leading to less NPV mainly due to the decrease on oil production. However, although NPV decreases as permeability decreases, the critical slug size of 20 mole/day/segment remains the same for the rich gas condensate fluid when the DME ratio is above 0.6 in the mixture in the cases with different reservoir permeabilities. The highest NPV appears above critical slug size but would slowly decrease when the total DME amount is too high. Therefore, the optimum NPV is around critical slug size and with DME ratio above 0.6.

### 5.2 Future Work

In this study, only NPV with one-time DME injection is investigated. Considering the impact of reinjection with certain amount of DME on gas production and the injection cycles on gas production, it is necessary to design further case studies to evaluate the comprehensive effect on NPV.

# Reference


Al-Anazi, H., Walker, J., Pope, G., Sharma, M., and Hackney, D. 2005. "A Successful Methanol Treatment in a Gas/Condensate Reservoir: Field Application." SPE-80901-PA, 20(01): 60-69 https://doi.org/10.2118/80901-PA.

Bang, V., Pope, G., Sharma, m., Baran, J., and Ahmadi, M. 2010. "A New Solution To Restore Productivity of Gas Wells With Condensate and Water Blocks." *SPE-116711-PA*,13(02): 323-331. https://doi.org/10.2118/116711-PA.

Bang, V., Yuan, C., Pope, G., Sharma, M., Baran, J., Skildum, J., Linnemeyer, H. 2008. "Improving Productivity of Hydraulically Fractured Gas Condensate Wells by Chemical Treatment." In *OTC-19599-MS*. OTC: Offshore Technology Conference, 5-8 May, Houston, Texas, USA. https://doi.org/10.4043/19599-MS.

Bang, V., Pope, G., Sharma, M. 2010. "Phase-Behavior Study of Hydrocarbon/Water/Methanol Mixtures at Reservoir Conditions." *SPE-102100-PA*, 15(04): 959-968. https://doi.org/10.2118/102100-PA.

Bertoncello, A, Wallace, J., Blyton, C., Honarpour, M., Kabir, S. 2014. "Imbibition and Water Blockage In Unconventional Reservoirs: Well-Management Implications During Flowback and Early Production." *SPE-167698-PA*, 17(04): 497-506. https://doi.org/10.2118/167698-PA.

Chang, Y. 1990. "Development and Application of an Equation of State Compositional Simulator." Ph.D dissertation, The University of Texas at Austin.

CMG. 2016. *Winprop User's Guide*. Computer Modeling Group Ltd.

Dindoruk, B. 2012. "Development of a Correlation for the Estimation of Condensate to Gas Ratio (CGR) and Other Key Gas Properties From Density Data." In *SPE-160170-MS*. SPE: Society of Petroleum Engineers. Annual Technical Conference and Exhibition, 8-10 October, San Antonio, Texas, USA https://doi.org/10.2118/160170-MS.

Ganjdanesh, R., Rezaveisi, M., Pope, G., and Sepehrnoori, K. 2016. “Treatment of Condensate and Water Blocks in Hydraulic-Fractured Shale-Gas/Condensate Reservoirs.” *SPE-175145-PA*, 21(02): 665-674. https://doi.org/10.2118/175145-PA.

Gupta, S. 2009. “Unconventional Fracturing Fluids for Tight Gas Reservoirs.” In *SPE-119424-MS*. SPE: Society of Petroleum Engineers, Hydraulic Fracturing Technology Conference, 19-21 January, The Woodlands, Texas. https://doi.org/10.2118/119424-MS.

Khan, S.A., Pope, G. and Sepehrnoori, K. 1992. “Fluid Characterization of Three-Phase CO2/Oil Mixtures.” In *SPE-24130-MS*. SPE: Society of Petroleum Engineers, SPE/DOE Enhanced Oil Recovery Symposium, 22-24 April, Tulsa, Oklahoma. https://doi.org/10.2118/24130-MS.

“Market Outlool for Dimethyl Ether.” 2002. Topical report. Allentown, Pennsylvania: Air Products and Chemicals, INC.

Meng, X., and Sheng, J. 2016. “Optimization of Huff-n-Puff Gas Injection in a Shale Gas Condensate Reservoir.” *Journal of Unconventional Oil and Gas Resources* 16 (December): 34–44. https://doi.org/10.1016/j.juogr.2016.09.003.

Michelsen, M. 1980. “Calculation of Phase Envelopes and Critical Points for Multicomponent Mixtures.” *Fluid Phase Equilibria* 4 (1): 1–10. https://doi.org/10.1016/0378-3812(80)80001-X.

Neshat, S., Okuno, R. and Pope, G. 2018. “Simulation of Water and Condensate Blockage and Solvent Treatments in Tight Formations Using Coupled Three-Phase Flash and Capillary Pressure Models.” In *SPE-190242-MS*. SPE: Society of Petroleum Engineers, SPE Improved Oil Recovery Conference, 14-18 April, Tulsa, Oklahoma, USA. https://doi.org/10.2118/190242-MS.

Neshat, S., and Pope, G. 2017. “Compositional Three-Phase Relative Permeability and Capillary Pressure Models Using Gibbs Free Energy.” In *SPE-182592-MS*. SPE: Society of Petroleum Engineers, Reservoir Simulation Conference, 20-22 February, Montgomery, Texas, USA. https://doi.org/10.2118/182592-MS.

Pedersen, K. S., P. L. Christensen, and J. A. Shaikh. 2014. *Phase Behavior of Petroleum Reservoir Fluids, Second Edition*. CRC Press.

Peng, D., and Robinson, D. 1976. "A New Two-Constant Equation of State." *Industrial & Engineering Chemistry Fundamentals* 15 (1): 59–64. https://doi.org/10.1021/i160057a011.

Perschke, D. R. 1988. "Equation of State Phase Behavior Modeling for Compositional Simulation." Ph.D dissertation, The University of Texas at Austin.

Pope, G.A., Wu, W., Narayanaswamy, G., Delshad, M., Sharma, M. and Wang, P. 2000. "Modeling Relative Permeability Effects in Gas-Condensate Reservoirs With a New Trapping Model." *SPE-62497-PA*, 3(02): 171-178. https://doi.org/10.2118/62497-PA.

Ratnakar, R., Dindoruk, B. and Wilson, L. 2017. "Phase Behavior Experiments and PVT Modeling of DME-Brine-Crude Oil Mixtures Based on Huron-Vidal Mixing Rules for EOR Applications." *Fluid Phase Equilibria* 434 (February): 49–62. https://doi.org/10.1016/j.fluid.2016.11.021.

Redlich, O., and Kwong, J. 1949. "On the Thermodynamics of Solutions. V. An Equation of State. Fugacities of Gaseous Solutions." *Chemical Reviews* 44 (1): 233–44. https://doi.org/10.1021/cr60137a013.

Sayed, M., Liang, F. and Ow, H. 2018. "Novel Surface Modified Nanoparticles for Mitigation of Condensate and Water Blockage in Gas Reservoirs." In *SPE-189959-MS*. SPE: Society of Petroleum Engineers. International Conference and Exhibition on Formation Damage Control, 7-9 February, Lafayette, Louisiana, USA. https://doi.org/10.2118/189959-MS.

Soave, G. 1972. "Equilibrium Constants from a Modified Redlich-Kwong Equation of State." *Chemical Engineering Science* 27 (6): 1197–1203. https://doi.org/10.1016/0009-2509(72)80096-4.

Standing, M.B. 1977. *Volumetric and Phase Behavior of Oil Field Hydrocarbon Systems*. Society of Petroleum Engineers; Oversize Trade Pbk, glued bdg edition.

van der Waals. 1873. “On the Continuity of the Gas and Liquid State.” Ph.D dissertation, Leiden.

Yuan, C., and Pope, G. 2011. “A New Method to Model Relative Permeability in Compositional Simulators to Avoid Discontinuous Changes Caused by Phase Identification Problems.” In *SPE-142093-MS*. SPE: Society of Petroleum Engineers, Reservoir Simulation Symposium, 21-23 February, The Woodlands, Texas, USA. https://doi.org/10.2118/142093-MS.